

Accounts

Recent Progress of Functional Glycoconjugated Metal Complexes

Shigenobu Yano* **and Yuji Mikata†**

Division of Material Science, Graduate School of Human Culture, Nara Women's University, Kitauoyanishimachi, Nara 630-8506

†KYOUSEI Science Center, Nara Women's University, Kitauoyanishimachi, Nara 630-8506

(Received January 22, 2002)

Synthesis, characterizations and stereochemistry of the transition metal complexes containing glycosylamines derived from sugar molecules and polyamines have been investigated. During this study, the intelligent sugar complexes having ion recognition ability, novel sugar transformation reactions promoted by a cooperative effect of calcium ion and monoamines have been discovered. The biological activity of these metal complexes was also investigated. Antifungal nickel(II) complexes derived from amino sugars, and unprecedented sugar-dependent in vivo antitumor activity of carbohydrate-pendant cis-platinum(II) complexes are described in this article. These results suggested that the stereostructure and bioactivity of the sugar-metal complexes can be modified by varying amines and metal ions, and sugar molecules used.

Carbohydrates have a wide spread occurrence in nature and are indispensable compounds to living organisms. They are the constitutional parts of complex lipids (glycolipids) and proteins (glycoproteins). They are also building blocks of nucleotides and, hence, of nucleic acids and of the chemical ADP/ATP energy storage system. Thus, carbohydrates perform a wide range of functions in living organisms. On the other hand, metal ions are also indispensable for living systems. Due to the wide distribution of metals and their functions for all forms of life, metal-carbohydrate interactions are a key component for understanding bioinorganic chemistry. Study of complexation of carbohydrates to metals is one of the main objectives of carbohydrate coordination chemistry. Carbohydrates as ligands are very interesting in coordination chemistry and in bioinorganic chemistry in connection with metal-containing enzymes. Although it has been well known that sugars form complexes with transition metals, the field of interaction of sugars and their related compounds with metal is still largely unexplored, owing mainly to the multifunctionality, hygroscopic nature, and complicated stereochemistry of carbohydrates, and their relatively low coordination ability to metal ions.

Starting in 1966,[1] several reviews describing sugar metal complexes were published, among them the "classics" from Angyal.[2,3] Recent reviews by Vèrchere and co-workers[4] and by Alekseev and co-workers[5] discuss carbohydrate-metal complexes in solution and complexes of natural carbohydrates with metal cations, respectively. Whictfield, Stojkvski and Sarker,[6] Piarulli and Floriani,[7] and Gyurcsik and Nagy[8] reviewed mainly carbohydrate complexes of transition metals. Steinborn and Junicke[9] reviewed carbohydrate complexes of platinum group metals. Previously one of the authors has reviewed transition metal complexes containing *N*-glycoside[10] and sugar-metal interactions.[11] This account describes our recent studies of the synthesis, characterizations, and stereochemistry of the transition metal complexes (Ni^{2+},[12–14] Co^{2+},[15,16] Co^{3+},[17,18] $Mn^{II}Mn^{III}Mn^{II}$,[19–21] and Zn^{2+},[22]) containing sugar moieties, novel isomerizations of carbohydrates promoted by calcium ion and monoamines,[23] antifungal nickel(II) complexes derived from amino sugars[24,25] and antitumor activity of carbohydrate-pendant *cis*-platinum(II) complexes.[26] It includes those papers which were published from 1994 to the end of November 2001.

1. Stereochemistry and Circular Dichroism of Nickel(II) Complexes with *N*-Glycoside Ligands from Aldopentoses and 1,3-Diaminopropane[13]

We have systematically studied the syntheses and characterizations of metal complexes containing glycosylamines derived from the reactions between sugars and polyamines.[27–55] In the series of aldohexose-based mononuclear nickel(II) complexes, two tridentate *N*-aldosyldiamine ligands are coordinated in meridional mode to complete a *cis*-(*O*,*O*)-Ni[NNO]$_2$ octahedron, in which all sugar moieties adopt β-aldopyranosyl-$^4C_1$ structures.[27,29,31,32,34,41–45,54,55] The coordination modes of the sugar parts are classified into two types denoted as the *trans*-chelation form of D-glucose (D-Glc), D-galactose (D-Gal), and L-fucose (L-Fuc) and the *cis*-chelation form for D-mannose (D-

Man), D-talose (D-Tal), and L-rhamnose (6-deoxy-L-mannose) (L-Rha), on the basis of the crystal structure of [Ni(L-Rha-tn)$_2$]Br$_2$·2H$_2$O·CH$_3$OH (tn = 1,3-diaminopropane) and their circular dichroism spectral patterns (Scheme 1). In the *trans*-chelation form, the sugar pyranoid ring is coplanar with the five-membered chelate ring whereas in the *cis*-chelation form, the sugar ring is considerably tilted with respect to the chelate ring.

Aldopentoses, in general, show more flexible conformational structures in comparison with aldohexoses, mainly due to the absence of a C-6 hydroxymethyl group, which leads to complicated stereochemistry around a metal center. Reactions of [Ni(tn)$_3$]X$_2$·2H$_2$O (X = Cl or Br) with aldopentoses afforded a series of mononuclear nickel(II) complexes with *N*-glycosylamine ligands, [Ni(aldose-tn)$_2$]X$_2$ [aldose-tn = 1-(*N*-aldosyl)-amino-3-aminopropane, aldose = D-xylose (D-Xyl) **1**, D-lyxose (D-Lyx) **2**, D-ribose (D-Rib) **3**, or D-arabinose (D-Ara) **4**]. The most salient feature for the crystal structure of compound **4b**, where X = Br, is that the sugar units adopt an unusual α-$^1C_4$-chair pyranoid conformation. This is the first example of metal-*N*-glycosylamine complexes in which an aldose binds to an amino group through an α-*N*-glycosidic linkage. The coordination behavior of D-ribose was confirmed by an X-ray analysis of an analogous compound, [Ni(D-Rib-men)$_2$]Br$_2$·2CH$_3$OH **5** [D-Rib-men = 1-methylamino-2-(*N*-D-ribosyl)aminoethane], derived from the reaction of [Ni(men)$_3$]Br$_2$ with D-ribose [men = 1-amino-2-(*N*-methylamino)ethane]. The D-ribose moiety forms an α-*N*-glycosidic bond with the primary amino group of men, and adopts an α-$^4C_1$ chair-form, the sugar chelate ring conformation being δ.

In general, the D-arabinosylamine moiety in the pyranose form is able to chelate to a metal in three different modes: (*cis*-δ)(β-$^4C_1$), (*trans*-δ)-(α-$^1C_4$), and (*cis*-λ)-(β-$^1C_4$), as shown in Fig. 1. The α-$^4C_1$ form is not suitable for chelation. In these structures, the α-$^1C_4$ form is seemingly the most thermodynamically stable and, in fact, the (*trans*-δ)-*R*-(α-$^1C_4$) mode is observed in the crystal structure of complex **4b**. The CD spectral features are in good accord with the crystal structure (Fig. 2). The spectral pattern was classified as a *trans*-chelation type and the sign of the Cotton effect around the first d–d transition band (8000–14000 cm^{-1}) varied from (−) to (+) with increasing wave-number, suggesting that the sugar-chelate ring conformation is δ and the absolute configuration of the *N*-glycosidic nitrogen atom is *R*. The absolute configuration of the *N*-glycosidic nitrogen atom depends on the conformation of the sugar-chelate ring in the event that the six-membered diamine chelate ring adopts a stable chair conformation.

The CD spectral patterns of the other complexes **1b** (D-xylose, Xyl) and **2b** (D-lyxose, Lyx) are also characteristic of the *trans*-sugar-chelation type (Fig. 2). As to the D-ribose complex **3b**, the CD spectrum could be recognized as of a *cis*-sugar-chelation type, and is indeed, quite similar to that of [Ni(L-Rha-tn)$_2$]Br$_2$ **6** which has a *cis*-λ sugar chelation.[54] The structural parameters are summarized in Table 1.

In addition, we have newly found that the sign of Cotton effect in 35000–45000 cm^{-1} region exclusively reflects the absolute configuration around the metal center; this was clear from a compilation of crystal structures and CD spectra of analogous compounds, [Ni(D-GlcN-tn)$_2$]Cl$_2$ **8**[25] (D-GlcN-tn = 1-{(3-aminopropyl)amino}-2-amino-1,2-dideoxy-D-glucose)

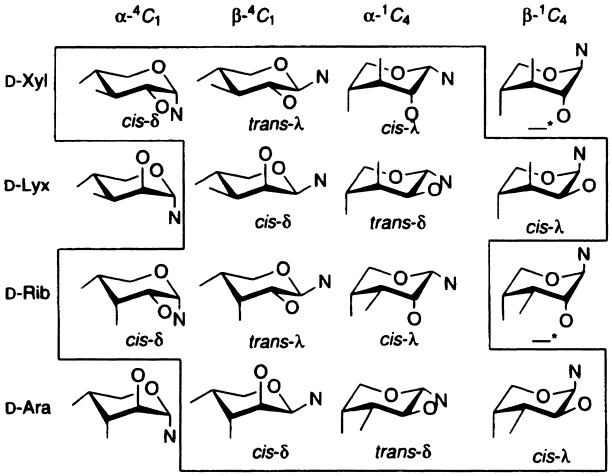

Fig. 1. Sugar pyranoid conformations which are able to chelate to a metal center.

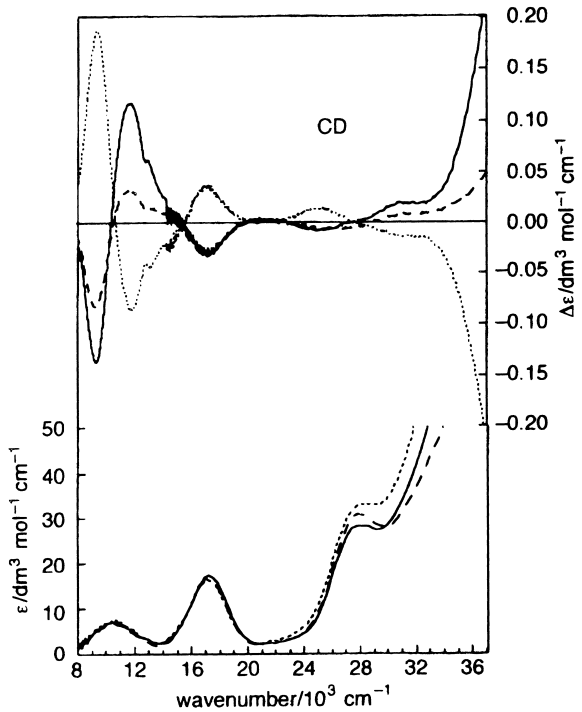

Fig. 2. Electronic absorption and circular dichroism spectra of [Ni(D-Xyl-tn)$_2$]Br$_2$ **1b** (·····), [Ni(D-Lyx-tn)$_2$]Br$_2$ **2b** (- - - - -), and [Ni(D-Ara-tn)$_2$]Br$_2$ **4b** (———) in methanol around d–d transition band region (8000–35000 cm^{-1}).

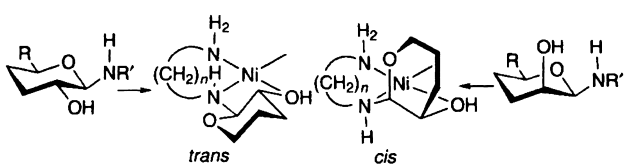

Scheme 1. R = CH$_2$OH, R′ = (CH$_2$)$_n$NH$_2$, n = 2 or 3.

Table 1. Structural Prameters for C_2 Symmetrical Nickel(II) Complexes Containing Two Tridentate *N*-Glycosylamine Ligands

	Complex	Absolute configuration around metal	Sugar chelation and its conformation	Configuration of *N*-glycosidic N atom	Sugar pyranoid conformation
6	[Ni(L-Rha-tn)$_2$]Br$_2$[a)]	Δ	*cis*-λ	*S*	β-$^4C_1$
7	[Ni(Mal-tn)$_2$]Cl$_2$[a)]	Δ	*trans*-λ	*S*	β-$^4C_1$[b)]
8	[Ni(D-GlcN-tn)$_2$]Cl$_2$[a)]	Δ	*trans*-λ	*S*	β-$^4C_1$
9	[Ni(D-GlcN-en)$_2$]Cl$_2$[a)]	Λ	*trans*-λ	*S*	β-$^4C_1$
4b	[Ni(D-Ara-tn)$_2$]Br$_2$[a)]	Λ	*trans*-δ	*R*	α-$^1C_4$
1	[Ni(D-Xyl-tn)$_2$]$^{2+}$	Δ	*trans*-λ	*S*	β-$^4C_1$
2	[Ni(D-Lyx-tn)$_2$]$^{2+}$	Λ	*trans*-δ	*R*	α-$^1C_4$
3	[Ni(D-Rib-tn)$_2$]$^{2+}$	Δ	*cis*-λ	*S*	α-^{1}C$_4$
5	[Ni(D-Rib-men)$_2$]Br$_2$[a)]	Δ	*cis*-δ	*R*	α-^{4}C$_1$

a) Determined by X-ray crystallography. b) Structure for the reducing terminal sugar, the chelating sugar.

and [Ni(D-GlcN-en)$_2$]Cl$_2$ **9**[31] (D-GlcN-en = 1-{(2-aminoethyl)amino}-2-amino-1,2-dideoxy-D-glucose). The (+) sign at about 40000 cm^{-1} corresponds to the Λ configuration and the (−) sign to the Δ. This empirical rule is also consistent with the CD spectral sign at around 40000 cm^{-1} for the structurally characterized complexes **6**, **7** and **4b** (Table 1). In the light of this sign, **1** (D-Xyl), **2** (D-Lyx), and **3** (D-Rib) were assumed to have C_2 chiral configurations around the metal of Δ, Λ, and Δ, respectively. On the basis of the CD spectral signs, the C_2 chiral absolute configurations of [Ni(D-Glc-tn)$_2$]$^{2+}$ (D-GlcN-tn = 1-{(3-aminopropyl)amino}-1-deoxy-D-glucose) and [Ni(D-Gal-tn)$_2$]$^{2+}$ (D-Gal-tn = 1-{(3-aminopropyl)amino}-1-deoxy-D-galactose) reported in the literature[54] were reassigned as Δ.

2. Assembly of Aldoses on a Nickel(II) Center by Utilizing *N*-Glycosidic Bond Formation with Tris(2-aminoethyl)amine[12]

A branched polyamine, tris(2-aminoethyl)amine (tren), having three primary amino groups, was introduced to assemble three sugar units on the metal center in a symmetrical fashion. We wish to describe herein the assembly of aldoses on nickel(II) ion by utilizing the *N*-glycosidic bond formation with tren, mainly focusing on the syntheses and characterization of bis- and tris-sugar complexes, [Ni{*N*,*N*′-(aldosyl)$_2$-tren}]$^{2+}$ and [Ni{*N*,*N*′,*N*″-(aldosyl)$_3$-tren}]$^{2+}$.

Reactions of [Ni(tren)(H$_2$O)$_2$]X$_2$ (**10**) with D-mannose and L-rhamnose (6-deoxy-L-mannose), having 2,3-*cis* configuration, in the presence of a small amount of tren yielded bis-sugar nickel(II) complexes formulated as [Ni{*N*,*N*′-(aldose)$_2$-tren}]X$_2$ (aldose = D-Man, X = Cl (**11a**), Br (**11b**), X$_2$ = SO$_4$ (**11c**); aldose = L-Rha, X$_2$ = SO$_4$ (**12c**)). Electronic absorption (AB) and circular dichroism (CD) spectra for [Ni(*N*,*N*′-aldose)$_2$-tren]X$_2$ are shown in Fig. 3. The AB spectra consist of three principal bands with comparatively low intensities (< 30 M^{-1} cm^{-1}), which are also characteristic of octahedral nickel(II) complexes and are assigned to the three spin-allowed transitions: $^3A_{2g}(F) \rightarrow {}^3T_{2g}(F)$, $^3A_{2g}(F) \rightarrow {}^3T_{1g}(F)$, and $^3A_{2g}(F) \rightarrow {}^3T_{1g}(P)$.[56] The CD spectral patterns are almost mirror-imaged between **11** and **12**, which is consistent with the fact that D-mannose and L-rhamnose are enantiomeric except for C-6 hydroxyl groups.

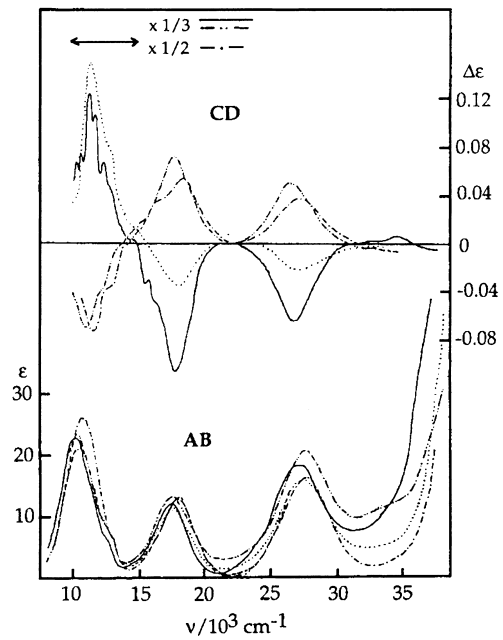

Fig. 3. UV-vis absorption (AB) and circular dichroism (CD) spectra of (a, —) [Ni(N,*N*′-(D-Glc)$_2$-tren)]Cl$_2$ (**13a**) in MeOH, (b, ·--) [Ni(*N*,*N*′-(D-Man)$_2$-tren)]Cl$_2$ (**11a**) in DMSO, (c, ····) [Ni(*N*,*N*′-(D-Man)$_2$-tren)]SO$_4$ (**11c**) in ethyleneglycol, and (d, - -)[Ni(*N*,*N*′ -(L-Rha)$_2$-tren)]SO$_4$ (**12c**) in MeOH/ethyleneglycol.

A perspective drawing of the complex cation of **11a** with the atomic numbering scheme is illustrated in Fig. 4. The salient feature is found in the interaction between the two sugar parts. The tetradentate tren ligand directs two mannose residues to the same side of the complex, resulting in the intramolecular sugar-sugar hydrogen bondings. The complex cation of **11a** can be divided into two blocks: a hydrophobic polyamine part and a hydrophilic sugar part, the latter involving distinct sugar–sugar hydrogen bonding interactions. Noncovalent interactions are vital in the processes of biological recognitions involving the enzyme-substrate, hormone-receptor, and antigen–antibody interactions. Thus, the structural feature of **11a** might give fundamental information in designing an artificial

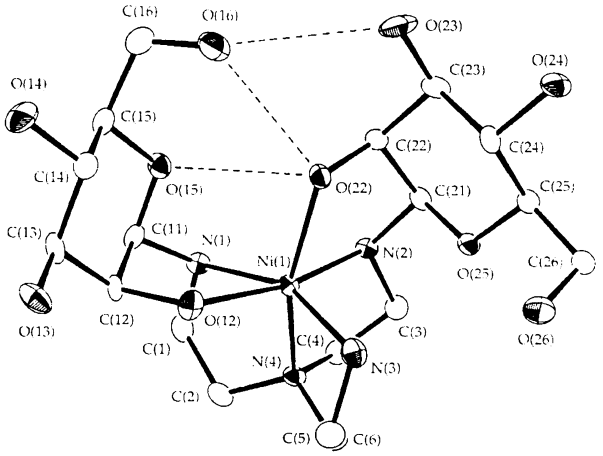

Fig. 4. ORTEP view of the complex cation of **11a**, [Ni(*N*,*N*′-(D-Man)$_2$-tren)]$^{2+}$.

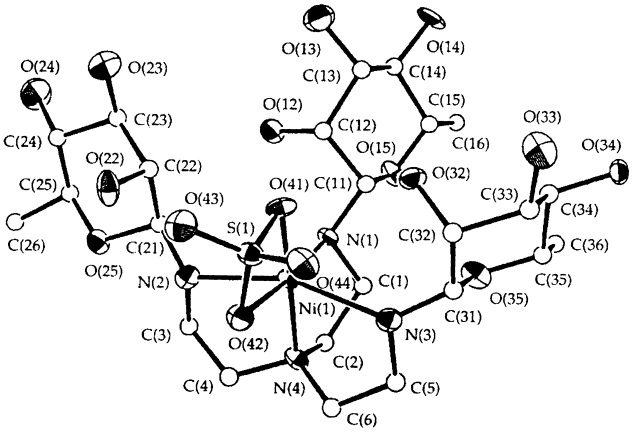

Fig. 5. ORTEP diagram of complex **19**, [Ni(*N*,*N*′,*N*″-(L-Rha)$_3$-tren)(SO$_4$)]. Carbon atoms are illustrated with arbitrary circle for clarity.

molecular recognition complex by utilizing carbohydrates.

Reaction of [Ni(tren)(H$_2$O)$_2$]Cl$_2$ (**10a**) with an excess of D-glucose, having 2,3-*trans* configuration, in the presence of a small amount of tren resulted in a formation of mono-sugar nickel(II) complex, [Ni{*N*-(D-Glc)-tren}(H$_2$O)]Cl$_2$·0.5H$_2$O (**13**·0.5H$_2$O), in low yield, and the bis-sugar complex, [Ni{*N*,*N*′-(D-Glc)$_2$-tren}]Cl$_2$ (**13a**), was not obtained. The similar reactions of **10a** with D-glucosamine (2-amino-2-deoxy-D-glucose, D-GlcN) and D-galactosamine (2-amino-2-deoxy-D-galactose, D-GalN) also gave the mono-sugar complex, [Ni{*N*-(D-GlcN)-tren}(H$_2$O)]Cl$_2$ and [Ni{*N*-(D-GalN)-tren}(H$_2$O)]Cl$_2$·H$_2$O. The analytical, magnetic, and electronic absorption spectroscopic data of these complexes indicated that the octahedral nickel(II) complex is ligated by a pentadentate *N*-glycoside ligand, (*N*-aldosyl-2-aminoethyl)bis(2-aminoethyl)amine.

Tris-sugar complexes formulated as [Ni{*N*,*N*′,*N*″-tri(aldosyl)-tren}]X$_2$ (aldose = D-mannose (**14**), L-rhamnose (**15**), D-glucose (**16**), maltose (Mal) (**17**), and melibiose (Mel) (**18**)) were prepared by the reaction of nickel(II) salts with *N*,*N*′,*N*″-tri(aldosyl)-tren ligands. The labile *N*,*N*′,*N*″-tri(aldosyl)-tren was prepared by the reaction between tren and aldose without metal ions, and could be stabilized by the coordination to a nickel(II) ion. Isolated and characterized compounds were [Ni{*N*,*N*′,*N*″-(D-Man)$_3$-tren}]X$_2$ (**14a**: X = Cl; **14b**: X = Br), [Ni{*N*,*N*′,*N*″-(L-Rha)$_3$-tren}]X$_2$ (**15a**: X = Cl; **15b**: X = Br), [Ni{*N*,*N*′,*N*″-(D-Glc)$_3$-tren}]Cl$_2$ (**16**), [Ni(*N*,*N*′,*N*″-Mal$_3$-tren)]-Br$_2$ (**17**), and [Ni{*N*,*N*′,*N*″-Mel$_3$-tren}]Br$_2$ (**18**). These complexes could not be obtained by the reactions of [Ni(tren)(H$_2$O)$_2$]$^{2+}$ (**10**) with excess amounts of aldoses. The AB spectra of these complexes consist of three principal bands with comparatively low intensities (< 30 M^{-1} cm^{-1}), characteristic of octahedral nickel(II) complexes. The tris-sugar nickel(II) complexes **14**, **15**, and **16**–**18** were assumed to have a C_3-symmetrical structure with the *N*,*N*′,*N*″-tri(aldosyl)-tren ligand, although the coordination of the tertiary nitrogen atom of tren is not clear. ^{13}C NMR spectra of **17** and **18** were measured to confirm the C_3-symmetrical structure.

The absolute configuration around the metal center (configurational effect) is the major contributor to the circular dichroism (CD) rather than the chelate ring conformation (conformational effect) and the chiral centers on the ligands (vicinal effect). The sign of the CD spectra is thus very informative as to the helical configuration. The CD spectra of **16**–**18** also exhibited plus-sign Cotton effects in the region of the first d–d transition band (10.5–10.9 k cm^{-1}), strongly suggesting that the C_3 helical configuration is Δ with a *lel* arrangement of three λ conformations comprising sugar moieties. The corresponding sign of the CD spectra of **14** is plus (11.0–11.1 k cm^{-1}), indicating Δ-δ_3 (*ob*) arrangement, which might be stabilized by hydrogen bonding interactions between the sugar moieties as observed in **11**. Complexes **15** were assumed to have the enantiomeric structure to **14**, Λ-λ_3 (*ob*), since the CD spectral pattern is almost the mirror image of those of **14**. When the reaction of *N*,*N*′,*N*″-(L-Rha)$_3$-tren with NiSO$_4$·6H$_2$O was carried out at low temperature instead, a neutral complex [Ni{*N*,*N*′,*N*″-(L-Rha)$_3$-tren}(SO$_4$)]·2H$_2$O (**19**·2H$_2$O) was isolated. The structure of **19** was determined by X-ray crystallography as shown in Fig. 5. Complex **19** comprises a fairly distorted octahedral nickel(II) cation ligated by a didentate sulfate anion and the *N*-glycoside ligand, *N*,*N*′,*N*″-tris(β-L-rhamnosyl)tren, which acts as a tetradentate ligand through the four nitrogen atoms. The sugar moieties are anchored on the metal center by only the glycosidic nitrogen atom on C-1 position; all hydroxyl groups of sugar residues being out of coordination although this ligand is potentially heptadentate. Complex **19** is able to be regarded as an intermediate species to the C_3 symmetrical trisugar complexes and, in fact, treatment of **19** with BaBr$_2$·2H$_2$O led to the formation of **15b**.

3. Unprecedented Chiral Inversion around a Seven-Coordinated Cobalt(II) Center Induced by an Interaction between Sugars and Sulfate anions[16]

A series of cobalt(II)-sugar complexes were prepared by the reactions of cobalt(II) salts, CoX$_2$·6H$_2$O (X = Cl, Br) and CoSO$_4$·7H$_2$O, with heptadentate *N*-glycoside ligands, (aldose)$_3$tren, which were derived from tren and D-mannose and from tren and L-rhamnose (6-deoxy-L-mannose). The electronic absorption spectra of complexes [Co{(aldose)$_3$-tren}]X$_2$·*n*H$_2$O (**20**–**22**) in solution showed a characteristic

band around 20000 cm^{-1}, corresponding to d–d transitions of Co(II) ions. In the circular dichroism spectra large Cotton effects were observed at about 20000 cm^{-1}, suggesting the coordination of sugar moieties to the cobalt ion. Further, it should be noted that the sign of the Cotton effect of **20** (X = Cl^-) and **21** (X = Br^-), containing halide counter anions, is opposite to that of **22**, containing the SO_4^{2-} counter anion. The opposite nature of the signs for **20** and **21** vs **22** was attributed to an inversion of the absolute configuration around the metal ion induced by counter anion. In fact, in light of the X-ray structures of L-rhamnose complexes **21b** and **22b** (Figs. 6 and 7), the opposite nature of the signs in the CD spectra for the halide and sulfate anions was interpreted as a configurational inversion around the cobalt center by the sulfate ion.

The structures of $[Co\{(D\text{-}Man)_3tren\}]^{2+}$ in the Δ and Λ configurations were assumed to be the mirror images of the corresponding structures of $[Co\{(L\text{-}Rha)_3tren\}]^{2+}$ because D-Man and L-Rha (6-deoxy-L-mannose) are almost enantiomeric to each other. It can be expected that $[Co\{(D\text{-}Man)_3tren\}]X_2$ (X = Cl^-, Br^-) has a Δ (δ_3-*ob*) helical configuration, which may be stabilized by an inter-ligand hydrogen bonding network, as observed in the structure description of **21b**. The observations of the nearly mirror images in the CD spectra between the D-mannose complexes and L-rhamnose complexes supported this structural assumption. In contrast, $[Co\{(D\text{-}Man)_3tren\}]SO_4$ adopts a Λ (δ_3-*lel*) configuration, where the SO_4^{2-} anion is probably fitted to the large-size shallow cavity at the facial site, as observed in the L-rhamnose complex **22b**.

The X-ray crystal structure of **22b**·$3H_2O$·CH_3OH and the CD spectra suggest ion-pair formation between the complex cation and the sulfate anion in solution. In order to confirm the presence of the ion pair in solution, we tried to estimate the closest distance of approach of ions on the basis of the EYY theory[57,58] for ion association, resulting in the most appropriate value of 5 Å in both the rhamnose and mannose complexes. This value is consistent with the Co–S distance of 4.697(6) Å determined by X-ray crystallography of **22b**·$3H_2O$·CH_3OH.

Complex **22b** was readily transformed into **21a**,**b** by the addition of BaX_2 (X = Cl, Br), and complexes **21a**,**b** were converted to **22b** by the addition of Na_2SO_4 as mentioned above. The configurational inversion around the metal ion thus proceeded reversibly, just as flowers open and close (Fig. 8). Here, we wish to consider why the novel chiral inversion between the halide salts and the sulfate salts occurred. The complexes $[Co\{(L\text{-}Rha)_3tren\}]X_2$ (**20b**, X = Cl^-; **21b**, X = Br^-) have Λ (λ_3-*ob*) helical configuration (**20a** and **21a**: Δ(δ_3-*ob*)). The facial site is blocked by the carbohydrate residues, resulting in a narrow, deep cavity. On the other hand, $[Co\{(L\text{-}Rha)_3tren\}]SO_4$ (**22b**) adopts a Δ(λ_3-*lel*) helical configuration (**22a**: Λ(δ_3-*lel*)), where the SO_4^{2-} anion is fitted to the wide,

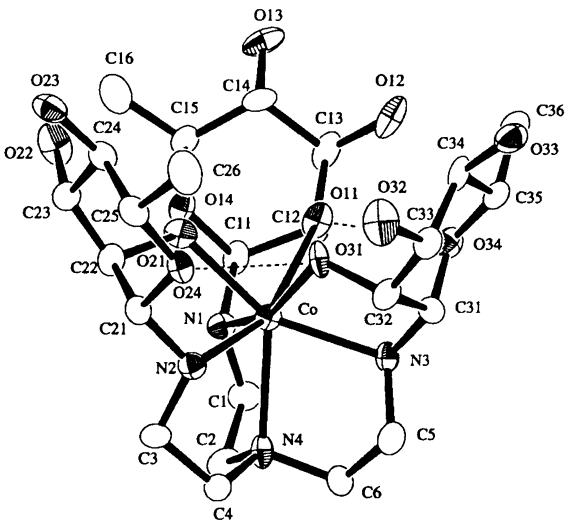

Fig. 6. ORTEP drawing of the complex cation **21b**, $[Co(L\text{-}Rha)_3tren]Br_2$.

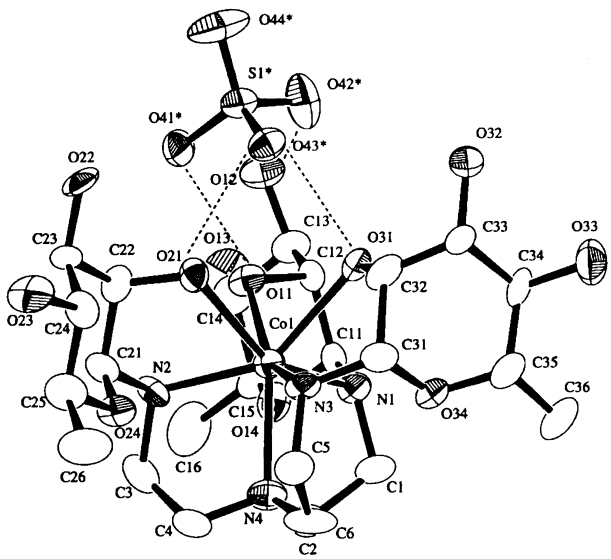

Fig. 7. ORTEP drawing of $[Co(L\text{-}Rha)_3tren]SO_4$ (**22b**).

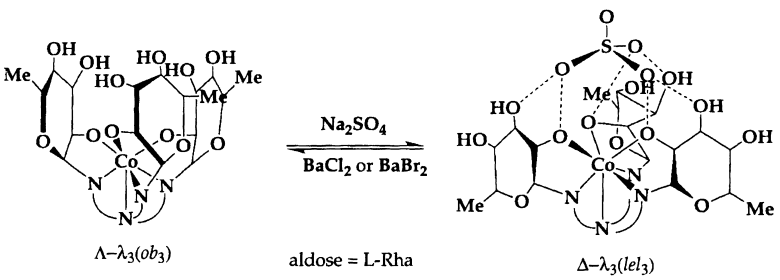

Fig. 8. Configurational inversion around the metal center in $[Co(L\text{-}Rha)_3tren]^{2+}$ induced by an interaction between sugars and SO_4^{2-}.

shallow cavity at the facial site. Generally, the *lel* form is more favorable than the *ob* form on the basis of CPK model. However, in our sugar complexes, the *ob* form may be stabilized by an interligand hydrogen-bonding network of the sugar units as is found in the crystal structure of **21b**·2CH_3OH.

The approach of the sulfate anion to the sugar complex cation due to the electrostatic attraction between the −2 charged sulfate ions and +2 charged complex cations cleaves the interligand hydrogen bonds and brings about a chiral inversion induced by the sulfate anion in the *lel* form fitting into the large, shallow cavity. The Λ-*lel* form will convert to the Δ-*ob* form again upon a removal of sulfate anions and an addition of barium(II) salts.

4. Peroxo-Bridged Dinuclear Cobalt(III) Complexes Containing *N*-Glycoside Ligands from Tris(2-aminoethyl)-amine and D-Glucose or Maltose[17,18]

This study was carried out by utilizing tren and D-glucose (D-Glc) and its disaccharide derivative maltose (Mal) as a sugar part. This 2,3-*trans* configuration and was equatorially oriented on ligating through the 1,2-functional groups with β-anomeric form (Scheme 2). The use of the glucose-type sugars has led to an entirely different chemistry from that of mannose-type sugars and resulted in successful isolation and characterization of novel μ-peroxo dicobalt(III) complexes supported by β-D-glycosyl polyamine ligand, where interligand sugar-sugar hydrogen bonds significantly deviate the $Co_2(\mu\text{-}O_2)$ core from planarity. Further, the clearly observed sugar-sugar interactions of the maltose complex might be of potential importance in relevance to sugar clusters of glycoproteins on the surfaces of cell membranes.

Cobalt(II) salts, $Co^{II}X_2$·6H_2O (X = Cl, Br), were treated with bis(*N*-D-glucosyl-2-aminoethyl)amine ((D-Glc)$_2$-tren), which was prepared from D-glucose (D-Glc) and tris(2-aminoethyl)amine (tren) in situ. The reaction mixture was bubbled by dioxygen or air for 4 h and was chromatographed on a Sephadex LH-20 gel permeation column eluted by methanol. Many bands were observed on the column chromatography, and the first-eluted, brown main band was collected. A slow evaporation of the solution yielded brown crystals formulated as [{Co[(D-Glc)$_2$-tren]}$_2$(μ-O_2)]X_3·5H_2O (X = Cl (**23**), Br (**24**)). A similar complex, [{Co[(Ma1)$_2$-tren]}$_2$(μ-O_2)]Cl_3·6H_2O (**25**), was also isolated, (Mal)$_2$-tren being bis(*N*-maltosyl-2-aminoethyl)(aminoethyl)amine. A reaction under nitrogen atmosphere prevented the formation of peroxo-bridged complex, indicating that the peroxo unit is derived from dioxygen, although the reactant of oxygen, presumably cobalt^{II}-*N*-glycoside complex, has not been isolated thus far. In the electronic absorption (AB) spectra, some intense electronic absorption bands (log ε 3.46–3.73) were observed around 400 nm, these are corresponding to a peroxo-metal charge-transfer band by analogy with peroxo-bridged cobalt(III) dinuclear complexes.[59] The IR peaks (**23** and **24**) at 888 cm^{-1} were also assignable to $\nu_{o\text{-}o}$ vibration.

We have previously demonstrated that deuterium isotope effects on ^{13}C NMR chemical shifts are very helpful in spectral assignments and confirmation of *N*-glycosidic bond formation.[46,50] Partial deuteriation of a coordinated NH_2 primary amino group, existing as NH_2, NHD, and ND_2 in a 1:2:1 ratio, causes ^{13}C resonances of α-carbons to appear as triplets, and that of a NHR secondary amino group, existing as NHR and NDR in a 1:1 ratio, to appear as doublets, since proton exchange of the coordinated amino groups is generally slow on the NMR time scale. The ^{13}C NMR spectrum of **24**·5H_2O in a D_2O/H_2O (1:1) mixed solvent was measured with a broadband decouple mode. The peaks for the anomeric carbon, Cl and Cl′, and α-carbons of tren, C2″, C4″, and C6″, are depicted in Fig. 9. The resonances for the C-1 carbon atoms of D-glucose (Cl and C1′) were observed at δ 93.50 and 93.21 as doublets owing to the isotope induced shifts of the neighboring N-H and N-D species. The observed isotope shifts, 95 ppb (C1) and 88 ppb (C1′), are comparable to the values reported as two bond effect.[46,50] These spectral features clearly demonstrated the presence of *N*-glycosidic bonds between two D-glucose molecules and tren. The resonances for the three methylene carbons (C2″, C4″, C6″) of tren also showed significant isotopic multiplets, two doublets at 50.39 and 48.11 ppm for C2″ and C4″ and a triplet at 45.84 ppm for C6″, which are consistent with an asymmetrical bis{*N*-(D-glucosyl)-2-aminoethyl}(2-aminoethyl)amine ligand. The observed two bond effects per deuterium ($^2\Delta$) are 131 ppb for C2″, 109 ppb for C4″, and 124 ppb for C6″. The ^1H NMR spectrum of **24**·5H_2O in DMSO-d_6 showed an extremely low-field shifted proton resonance at δ 12.64, which corresponds to the strongly hydrogen

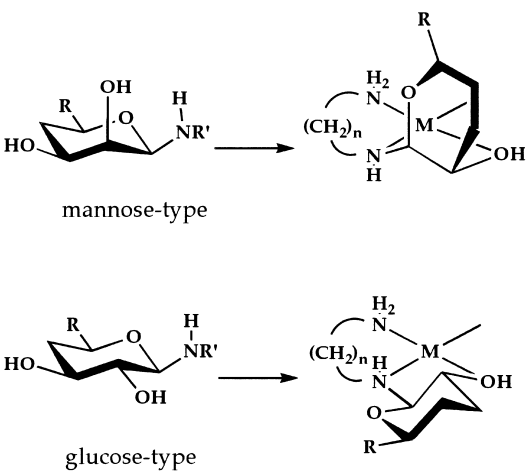

Scheme 2. R = CH_2OH, R′ = $(CH_2)_nNH_2$, n = 2 or 3.

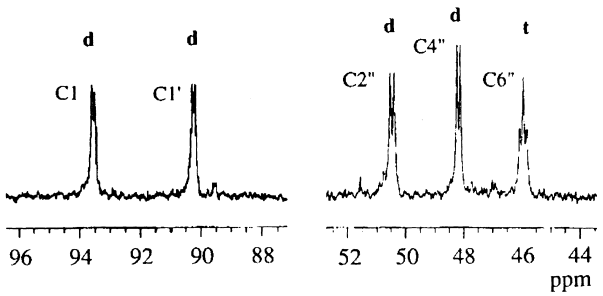

Fig. 9. ^{13}C {^1H} NMR spectrum of [{Co((D-Glc)$_2$-tren)}$_2$(μ-O_2)]Br_3·5H_2O (**24**·5H_2O) in D_2O/H_2O (1/1) for the α carbons with respect to amino groups.

bonded O–H···O$^-$ proton, as shown in the X-ray crystal structure of **23** (vide intra).

ORTEP diagrams for the complex cation of **23** are illustrated in Fig. 10. The complex cation consists of two Co(III) ions bridged by a peroxo unit (O(1)–O(2) = 1.452(10) Å). The cation has a pseudo C_2 symmetry with respect to an axis passing through the middle of the O–O bond. Each cobalt ion is ligated by the *N*-glycoside, (D-Glc)$_2$-tren, through the four nitrogen atoms and the C-2 oxygen atom of a sugar moiety together with the peroxide to form a distorted *cis*-(*O*,*O*)-[CoN_4O_2] octahedral geometry.

The similar structure of **25** is depicted in Fig. 11, where the structure of the dinuclear core **25**, except the nonreducing α-D-glucopyranosyl residues, is essentially identical to that of **23**. Two cobalt(III) octahedrons, ligated by a pentadentate (Mal)$_2$-tren ligand, are bridged by a peroxo unit. The average O–O distance of the peroxo units is 1.46 Å, and the avarage Co–Co interatomic distance is 4.100 Å. The average Co–O–O–Co torsion angle is deformed to 102°, supported by some interunit hydrogen bonds as observed in **23** [O(112)···O(312) = 2.45(2) Å, O(113)···O(313) = 2.69(2) Å].

To elucidate an electronic structural change by varying Co–O–O–Co torsional angle (θ), extended Hückel MO calculations were performed on a model compound, [*cis*-(*O*,*O*)-{$Co(NH_3)_4(H_2O)$}$_2$(μ-O_2)]$^{4+}$ (I) with C_2 symmetry. Figure 12 is an interaction diagram for I (θ = 180°) in terms of [{$Co(NH_3)_4(H_2O)$}$_2$]$^{6+}$ and O_2^{2-}, showing a large HOMO 2b (π^*_g)-LUMO lb (σ^*_u) gap of 2.8l eV, which accounts for the stability of (μ-peroxo)dicobalt(III) complexes.

A Walsh diagram with the Co–O–O–Co torsion angle θ varying from 180 to 70° is depicted in Fig. 13. The energy levels of the valence orbitals are almost independent of θ in the range of 180–95°, while the HOMO (2b) is slightly stabilized around $\theta \sim 100°$ owing to release of the antibonding interaction between the peroxo oxygen atoms. The unstabilization in the range of 95–70° is attributable to repulsive interaction between the water ligands of respective metal centers, which

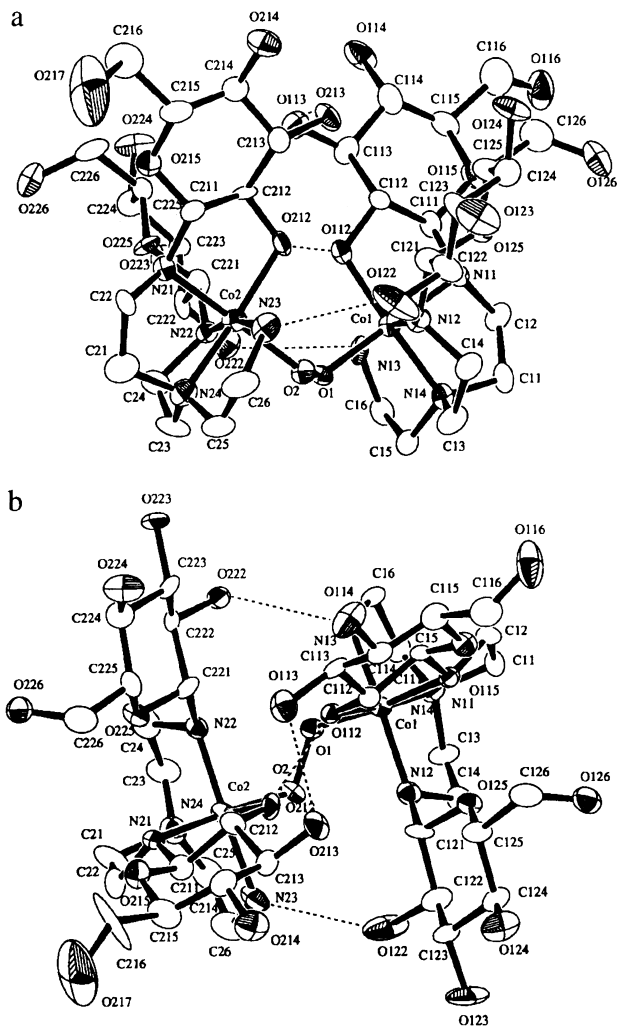

Fig. 10. ORTEP plots of the complex cation of **23**, [{Co((D-Glc)$_2$-tren)}$_2$(μ-O_2)]C1$_3$: (a) viewed vertical to the pseudo C_2 axis and (b) viewed along the pseudo C_2 axis.

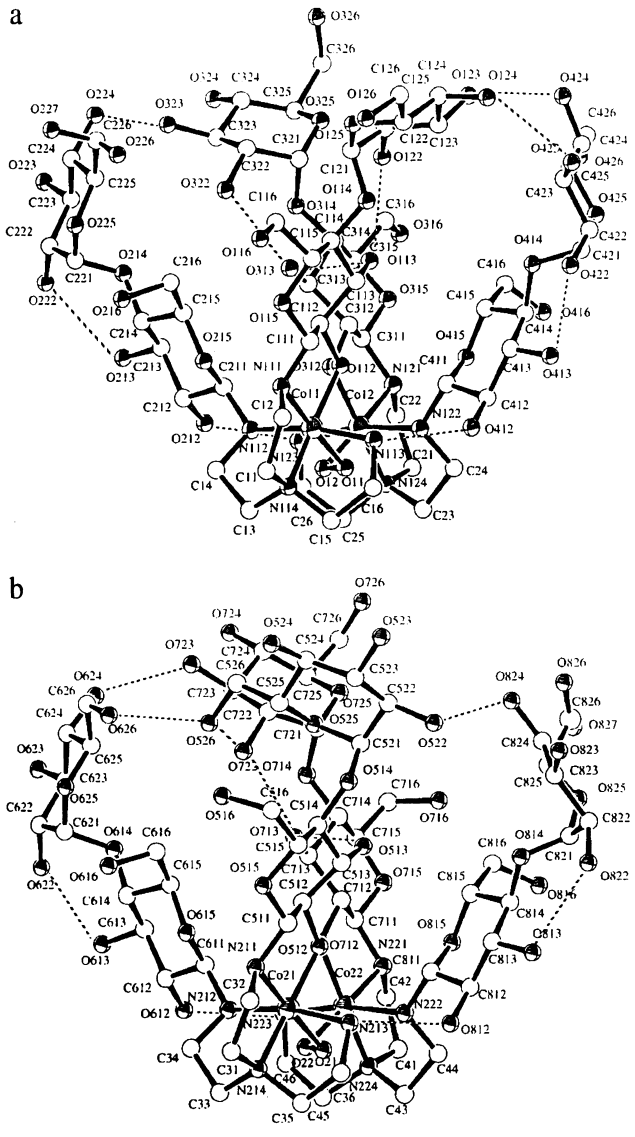

Fig. 11. ORTEP plots of the complex cation of **25**, [{Co((Mal)$_2$-tren)}$_2$(μ-O_2)]C1$_3$: (a) viewed vertical to the pseudo C_2 axis and (b) viewed along the pseudo C_2 axis.

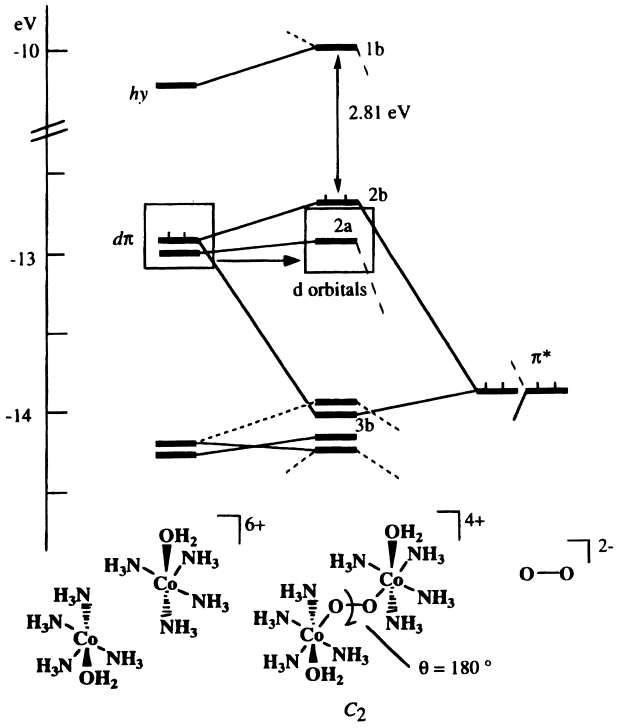

Fig. 12. MO interaction diagram for [*cis*-(*O*,*O*)-{$Co(NH_3)_4(H_2O)$}$_2$(μ-O_2)]$^{4+}$ in terms of 2 [$Co(NH_3)_4(H_2O)$]$^{3+}$ and O_2^{2-}. The torsional angle θ (Co–O–O–Co) is 180°.

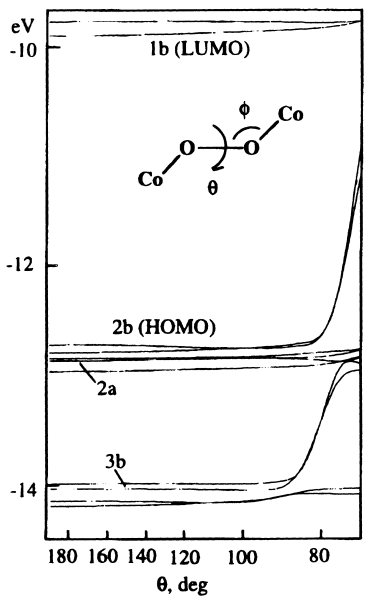

Fig. 13. Walsh diagram for the valence MO's of [*cis*-(*O*,*O*)-{$Co(NH_3)_4(H_2O)$}$_2$(μ-O_2)]$^{4+}$ by varying the torsional angle θ (Co–O–O–Co) from 180° to 70° with the Co–O–O angle (φ) being 117°.

should be avoided by the sugar-sugar hydrogen bonding [O(112)···O(212)] in **23** and **25**. These results strongly demonstrated that the observed unusually twisted structure (θ = 100–102°) in the Co_2(μ-O_2) core of **23** and **25** is ascribed to a combination of the slight electronic stabilization factor in the Co_2(μ-O_2) core and the sugar–sugar hydrogen bonding interaction.

5. $Mn^{II}Mn^{III}Mn^{II}$ Trinuclear Complexes with Carbohydrate Bridges Derived from Seven-Coordinate Manganese(II) Complexes with *N*-Glycoside[19,21]

Recent biological studies have shown the importance of dinuclear metal aggregations, in particular with Mn^{2+} and Mg^{2+} ions, in some enzymes and proteins handling sugar derivatives. Xylose isomerases promote aldose-ketose isomerization by utilizing a carboxylate-bridged dimetal center of Mg^{2+}, Mn^{2+}, or Co^{2+} ions in the active sites ~4.9 Å apart.[60,61] The similar dinuclear array of Mg^{2+} or Mn^{2+} in ~3.7 Å separation also promotes the cleavage of phosphate esters in fructose 1,6-bisphosphatase.[62,63] Concanavalin A, a lectin which specifically binds saccharides containing mannosyl residues, involves a pair of Ca^{2+} and Mn^{2+} ions bridged by an aspartate.[64] In this section, we describe the synthesis of mononuclear manganese(II) complexes of the heptadentate *N*-glycoside ligand that were converted into novel trimanganese complexes with a linear $Mn^{II}Mn^{III}Mn^{II}$ core bridged by an equatorial-axial-equatorial donor sequence of β-mannopyranosyl moieties.

Reactions of Mn(II) salts, $MnX_2{\cdot}nH_2O$, with tris(*N*-(D-mannosyl)-2-aminoethyl)amine ((D-Man)$_3$-tren), formed from tren and D-mannose in refluxing methanol, afforded colorless crystals formulated as [Mn((D-Man)$_3$-tren)]$X_2{\cdot}nH_2O$ (**26a**·$5H_2O$, X = Cl; **26c**·$4H_2O$, X = Br; **26c**·$4H_2O$, X = NO_3; **26d**·$4H_2O$, X = 1/2SO_4). Similar reaction of $MnSO_4{\cdot}5H_2O$ with tris(*N*-(L-rhamnosyl)-2-aminoethy1)amine, ((L-Rha)$_3$-tren), gave [Mn((L-Rha)$_3$-tren)]$SO_4{\cdot}4H_2O$ (**27d**·$4H_2O$). The elemental analysis showed a mononuclear manganese ion to be ligated by the potentially heptadentate *N*-glycoside ligand, (aldose)$_3$-tren, and the effective magnetic moments (5.62–5.89 μ_B) indicated the high-spin Mn(II) state. The X-ray crystallographic analyses of **26b** and **27d** indicated that complexes **26a–d** and **27d** are seven coordinate mononuclear Mn(II) complexes ligated by the (aldose)$_3$-tren *N*-glycoside ligand through [N_4O_3] donor atoms (vide infra).

When complexes [Mn((D-Man)$_3$-tren)]$X_2{\cdot}nH_2O$ (**26a**·$5H_2O$, X = C1; **26b**·$4H_2O$ [Mn((L-rha)$_3$-tren)]$SO_4{\cdot}4H_2O$ (**27d**·$4H_2O$)) were treated with 0.5 equiv of the corresponding Mn(II) salt, $MnX_2{\cdot}nH_2O$, in the presence of triethylamine, reddish orange crystals of [{Mn(aldose)$_3$tren)}$_2$Mn(H_2O)]$X_3{\cdot}nH_2O$ (**28a**·$6.5H_2O$, X = C1, aldose = D-Man; **28b**·$4H_2O$, X = Br, aldose = D-Man; **29d**·$7H_2O$, X = 1/2SO_4, aldose = L-Rha) were obtained in 20%, 26%, and 19% yields, respectively. Complexes **28a**, **28b**, and **29d** were shown by X-ray crystallography to be novel $Mn^{II}Mn^{III}Mn^{II}$ mixed valence trimanganese complexes with the (aldose)$_3$-tren ligand (vide infra). In the absence of Et_3N, the color of the reaction solution did not change and no crystalline compounds were isolated from the solution. Treatment of $MnX_2{\cdot}nH_2O$ with Et_3N, without the presence of the Mn(II)-sugar complexes, led exclusively to deposition of MnO_2 from methanolic solution. These results demonstrated that the added Mn(II) ion was encapsulated between two mononuclear Mn(II) complexes (**26**, **27**) and the trapped central Mn(II) ion was further oxidized to Mn(III) under aerobic conditions by the action of Et_3N to form the stable $Mn^{II}Mn^{III}Mn^{II}$ complexes (**28**, **29**). When the reactions were

carried out under nitrogen, formation of the $Mn^{II}Mn^{III}Mn^{II}$ complexes was dramatically suppressed, suggesting that dioxygen was an oxidant. Unfortunately, we have not been successful in isolating the postulated Mn^{II}_3 species, which might be more structurally relevant to xylose isomerases, despite some attempts to do so. The terminal Mn(II) centers were not oxidized during the reaction because they are sterically protected by the heptadentate cage-type *N*-glycoside ligand.

Reactions of $MnX_2 \cdot nH_2O$ with (L-Rha)$_3$-tren yielded a series of trimanganese complexes, [{Mn((L-Rha)$_3$-tren)}$_2$-Mn(H_2O)]$X_3 \cdot nH_2O$ (**29a**·11H_2O, X = C1; **29b**·10H_2O, X = Br; **29c**·8H_2O, X = NO_3), in 31–43% yields. When L-Rha was used as a sugar source, no mononuclear Mn(II) complexes with a (L-Rha)$_3$-tren ligand, the intermediate species postulated for the trimanganese complexes, were isolated, suggesting that Mn(II) complexes with (L-Rha)$_3$ tren are more unstable and/or reactive toward metal assembling than the corresponding isolated complexes with (D-Man)$_3$-tren (**26a–c**).

The trimanganese-sugar complexes (**28a**,**b** and **29a**,**d**) were assumed to have almost identical structures on the basis of IR spectra and electronic absorption and circular dichroism spectra and magnetic susceptibilities. The electronic absorption spectra of **28** and **29** in methanol showed a characteristic band around 470–505 nm ascribable to a Mn(III)-ligand charge transfer band, and appreciable Cotton effects were observed in the same region of the CD spectra, indicating that the Mn(III) center was ligated by chiral sugar moieties. The CD spectral patterns of complexes **28**, involving D-mannose residues, are almost mirror images of those of complexes **29** with L-rhamnose (6-deoxy-L-mannose) moieties, with respect to the $\Delta\varepsilon$ = 0 line.

Values of μ_{eff} at room temperature range from 8.46 to 9.28 μ_B, μ_{eff} per metal being 4.88–5.36 μ_B; such values are smaller than those of the Mn(II)-sugar complexes **26** and **27** (5.62–5.89 μ_B). Variable-temperature magnetic susceptibility data (4–300 K) were measured for complexes **29a–e**. The Hamiltonian, $H = -2[J_{12}S_1 \cdot S_2 + J_{23}S_2 \cdot S_3 + J_{13}S_1 \cdot S_3] + \mu_B [g_1S_1 + g_2S_2 + g_3S_3] \cdot B$, was employed in the analysis of the magnetic data, where $S_1 = S_3 = 5/2$, $S_2 = 2$, $J_{12} = J_{23} = J$, $J_{13} = J'$, and $g_1 = g_2 = g_3 = g$. The data were fit as the molar magnetic susceptibility to Eq. 1, which is derived from the field independent Van Vleck equation.

$$\chi_M = (N_g{}^2\mu_B{}^2/3kT)[\Sigma_i(S_i + 1)(2S_i + 1) \exp(-E_i/kT)]/[\Sigma_i(2S_i + 1) \exp(-E_i/kT)] \quad (1)$$

The exchange energies (E_i) were calculated by Kambe's method.[65,66] The best fits were obtained when J, J', and g were allowed to vary simultaneously, refining to values of J = -1.3 cm^{-1} (**29a**), -1.2 cm^{-1} (**29b**), -1.4 cm^{-1} (**29c**), J' = 0.3 cm^{-1} (**29a**), 0.3 cm^{-1} (**29b**), 0.2 cm^{-1} (**29c**), and g = 2.07 (**29a**), 1.95 (**29b**), 1.97 (**29c**). The values of J (-1.2 to -1.4 cm^{-1}) indicate that only weak antiferromagnetic coupling is mediated by the monodentate μ-alkoxo sugar bridging, and those of J' are negligible ($\sim$30) on the basis of relatively large zero-field splitting of Mn(II) ions.[67] The observed Mn(II)···Mn(III) antiferromagnetic interaction (Mn···Mn = 3.845 Å) is weaker than those found in the $Mn^{III}Mn^{II}Mn^{II}$ complexes (J = -3 to -7 cm^{-1} for Mn···Mn = 3.419–3.551 Å).

The structures of $Mn^{II}Mn^{III}Mn^{II}$ trinuclear complexes, **28a**, **28b**, **29c**, and **29d** were determined by X-ray crystallographic analyses. ORTEP drawings of the complex cations are depicted in Fig. 14 (**28b**) and 15 (**29d**). The complex cations have a pseudo C_2 symmetry and comprise a linearly ordered trimanganese core bridged by two carbohydrate residues (Fig. 14). The average Mn···Mn separations are 3.911(7) Å (**28a**) and 3.916(6) Å (**28b**), and the Mn···Mn···Mn angles are 171.0(1)° (**28a**) and 170.7(1)° (**28b**). The terminal Mn atoms are seven coordinate with a distorted mono-face-capped octahedral geometry ligated by the (D-Man)$_3$-tren ligand through three oxygen atoms of C-2 hydroxyl groups, three *N*-glycosidic nitrogen atoms, and a tertiary amino nitrogen atom. The geometrical and configurational aspects for the terminal Mn centers are essentially identical to those observed in [Mn((L-Rha)$_3$-tren)]SO_4 (**27d**); this strongly demonstrates the Mn(II) oxidation state for the terminal Mn ions in **28**. The C_3 helical configurations and the sugar chelate conformations are denoted as Λ-*lel*(δ_3), which is an inverted structure of Δ-*ob*$_3$(δ_3) found in [Mn((D-Man)$_3$-tren)]Br_2 (**26b**). Namely, an inversion of the Mn(II) center, from the Δ-*ob*$_3$ closed form to the Λ-*lel*$_3$ open form, could occur during the formation of **28a**,**b** from their precursors **26a**,**b**. The central Mn atoms are ligated by four

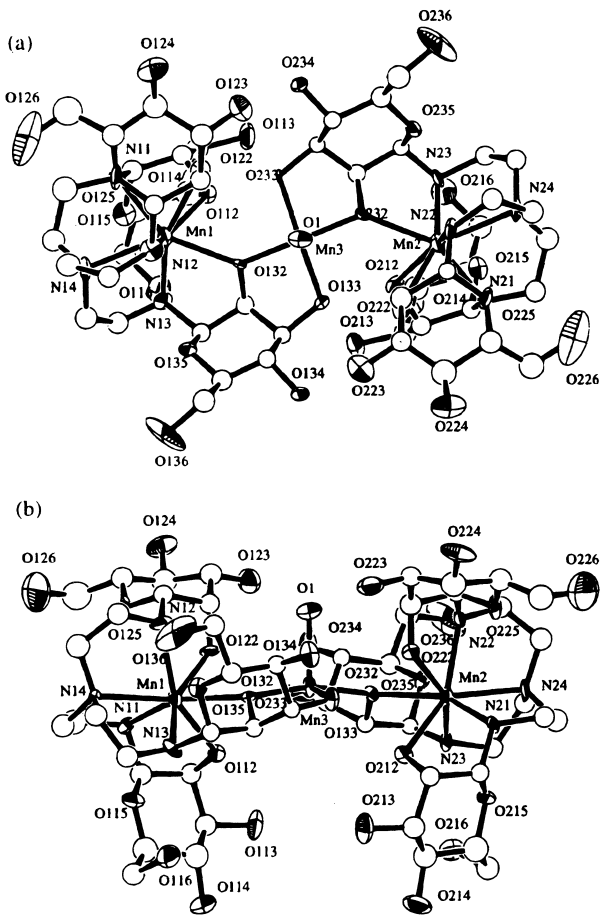

Fig. 14. ORTEP plots for the trimanganese cation of [{Mn((D-Man)$_3$-tren)}$_2$Mn(H_2O)]Br_3 (**28b**) (a) viewed along the pseudo C_2 axis and (b) viewed perpendicular to the axis.

oxygen atoms of bridging carbohydrate residues in the (D-Man)$_3$-tren ligands and one water molecule (2.19(1) Å for **28a** and 2.17(1) Å for **28b**), resulting in a square-pyramidal geometry.

On the basis of the bond lengths, the oxidation states of the central manganese atoms are assumed to be Mn(III). The C-2 and C-3 hydroxyl groups of the bridging sugar moieties are also estimated to be deprotonated from the short bond lengths to the central Mn atom 1.88(2)–1.96(2) Å for **28a** and 1.91(1)–1.93(1) Å for **28b**). The complex cations can also be viewed alternatively namely, the two seven coordinate Mn(II) complexes, $[Mn((D\text{-}Man)_3\text{-}tren)]^{2+}$, may trap a Mn(III) ion through a sugar domain. To our knowledge, the present trimanganese complex is the first example of $Mn^{II}Mn^{III}Mn^{II}$ linear assemblage, whereas many $Mn^{II}Mn^{II}Mn^{II}$ and $Mn^{III}Mn^{II}Mn^{III}$ compounds have already been reported.

The crystal structures of $[\{Mn((L\text{-}Rha)_3\text{-}tren)\}_2Mn(H_2O)]X_3$ (**29c**, X = NO_3; **29d**, X = 1/2SO_4) are isomorphous and have a crystallographically imposed C_2 symmetry with the axis passing through the Mn(1) and O(1) atoms. The structures of the complex cations are mirror images of **28a** and **28b**, except for the absence of C-6 hydroxyl groups of sugar units (Fig. 15).

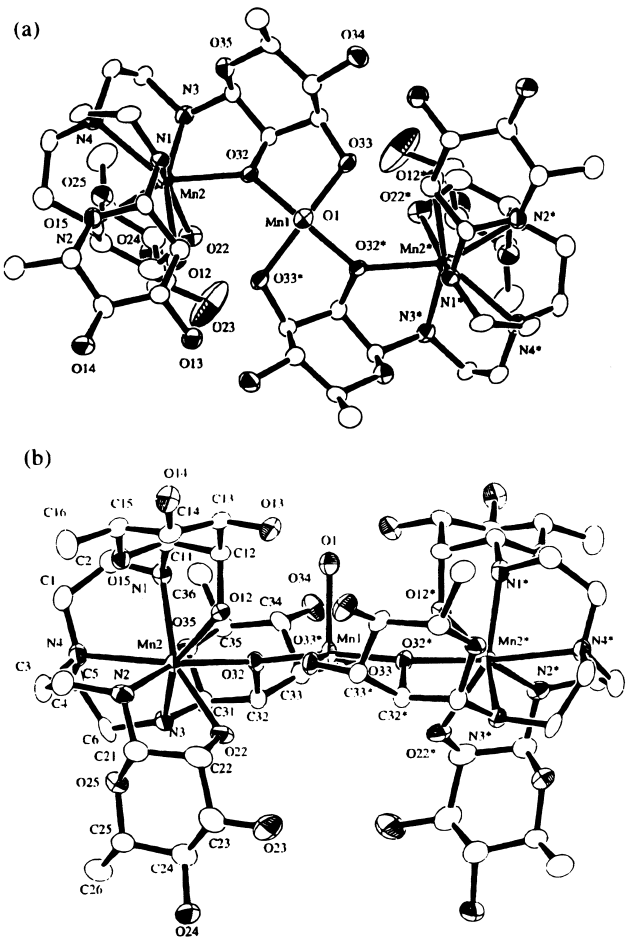

Fig. 15. ORTEP plots for the trimanganese cation of $[\{Mn((L\text{-}Rha)_3\text{-}tren)\}_2Mn(H_2O)](SO_4)_{1.5}$ (**29d**) (a) viewed along the C_2 axis and (b) viewed perpendicular to the axis.

The Mn···Mn separations are 3.845(2) Å (**29c**) and 3.855(1) Å (**29d**), and the Mn···Mn···Mn angles are 173.9(1)° (**29c**) and 173.81(7)° (**29d**). The metal-metal separations are shorter by ca. 0.06 Å than those observed in **28a** and **28b**. The structures around the terminal Mn(II) ions are almost identical to [Mn((L-Rha)$_3$-tren)]SO_4 (**27d**) with the Δ-*lel*(λ_3) configuration. The central Mn(III) atom is four-coordinate ligated by four oxygen atoms of bridging carbohydrate residues in the (L-Rha)$_3$-tren ligands (1.890(7), 1.920(8) Å for **29c** and 1.909(4), 1.920(6) Å for **29d**) and one water molecule (2.16(1) Å for **29c** and 2.203(8) Å for **29d**) in a square-pyramidal fashion.

The average O_{2b}–Mn(III)–O_{3b} and O_{2b}–Mn(II)–N^*_{sec} bite angles are 86.4° and 75.3°, respectively; these two five-membered chelate rings might bring about some strain in the six-membered pyranose ring. The observed C-2 alkoxo bridging mode on the dimanganese center is quite interesting in relation to the proposed mechanism of xylose isomerases which promote aldose-ketose isomerization by utilizing dimetal ions of Mg^{2+}, Mn^{2+}, and Co^{2+}.[60,61] In the proposed mechanism, an open-chain form aldose is fixed on the dimetal center (~4.9 Å apart) with a C-2 alkoxo bridge, which might be considered to activate the C–H bond on the C-2 position and promote a 1,2-hydride shift, a key step leading to ketose.[60,61]

6. Sugar Transformation by a Combination of Calcium Ion and Monoamines[23]

The formation of *N*-glycoside metal complexes with primary or secondary amines and sugar molecules were mainly described above. When tertiary amines and sugar derivatives were mixed in the presence of metal ion, C-2 epimerization was observed.[42,48] The transformation of sugar promoted by calcium ion is investigated in this chapter.

Many C-type animal lectin such as mannose-binding proteins require Ca^{2+} ions in their function[68] and selections also utilize Ca^{2+} ions to bind sialylated polysaccharides.[69,70] Concanavalin A, a lectin which specifically binds saccharides containing mannosyl residues, involves a pair of Ca^{2+} and Mn^{2+} ions bridged by aspartate near the sugar-recognition sites.[71] Previously, we have found that efficient C-2 epimerization of aldoses is promoted by nickel(II) and cobalt(II) complexes with *N*-substituted diamine ligands, *N*,*N*,*N*′-trimethylethylenediamine (*N*,*N*,*N*′-Me$_3$en) and *N*,*N*,*N*′*N*′-tetramethylethylenediamine (*N*,*N*,*N*′,*N*′-Me$_4$en), which proceed through a novel stereospecific rearrangement of the carbon skeleton or a pinacol-type 1,2-carbon shift.[37,39,45,48,53] Although similar C-2 epimerizations through a 1,2-carbon shift mediated by molybdate are also known,[72] the present reaction requires extremely mild conditions (5 min at 60 °C or 1 h at room temperature), where interactions between metal ions and diamines play crucial roles for the rearrangement. We have further extended the reaction by varying the metal ion and diamine components, aiming for biomimic functional transformations of carbohydrates. Here we describe aldose-aldose (C-2 epimerization) and aldose-ketose isomerizations of carbohydrates promoted by combination of Ca^{2+} and triethylamine, in which interesting substrate-dependent chemoselectivity is shown to arise from interaction of sugars with Ca^{2+} ions.

When various aldoses were used as the starting aldose in the reaction with Ca^{2+}-Et_3N in methanol, a conspicuous substrate-

Table 2. Isomerization of Various Aldoses Promoted by Combination of Ca^{2+} and Et_3N[a)]

Entry	Substrate	Yield of C-2 epimer (%)[b)]	Yield of ketose (%)[a)]	Recovery of substrate (%)[b)]
1	D-glucose	38	18	32
2	D-mannose	11	8	70
3	D-galactose	3	34	27
4	D-xylose	71	0	29
5	D-lyxose	9	0	75
6	D-arabinose	3	57	31
7	D-ribose	trace	0	85

a) Aldose (substrate) was treated with $CaCl_2 \cdot 2H_2O$ (1 equiv) and Et_3N (2 equiv) in methanol for 10 min at 60 °C. b) Determined by HPLC, based on the substrate.

dependent chemoselectivity was observed. The mannose-type aldoses having the 2,3-*erythro* configuration: D-mannose, D-lyxose, and D-ribose, significantly resisted both C-2 epimerization and ketose formation, presumably due to their stable complexation with Ca^{2+}. In particular, with C-2 epimers of D-xylose and D-lyxose, an almost complete substrate-selective C-2 epimerization (D-xylose, D-lyxose) was established by the Ca^{2+} and Et_3N system. Among the glucose-type aldoses having the 2,3-threo configuration, D-glucose, D-galactose, D-xylose, and D-arabinose, chemoselectivity between C-2 epimerization and ketose formation was observed, depending on the configurations of the starting aldoses (Table 2). The aldoses with 2,3-*threo* and 3,4-*threo* configurations, D-glucose and D-xylose, mainly underwent C-2 epimerization, and those having the 2,3-*threo* and 3,4-*erythro* configurations, D-galactose and D-arabinose, were mostly transformed into the corresponding 2-ketoses (Scheme 3). These features are of potential interest in relation to substrate selective isomerizations and transformations of carbohydrates catalyzed by metalloenzymes. ^{13}C NMR studies using D-(1-^{13}C)glucose and D-(1-^{13}C)galactose with the $CaCl_2$ system in CD_3OD revealed that the C-2 epimerization proceeds via stereospecific rearrangement of the carbon skeleton, or 1,2-hydride shift and, in part, via an enediol intermediate.

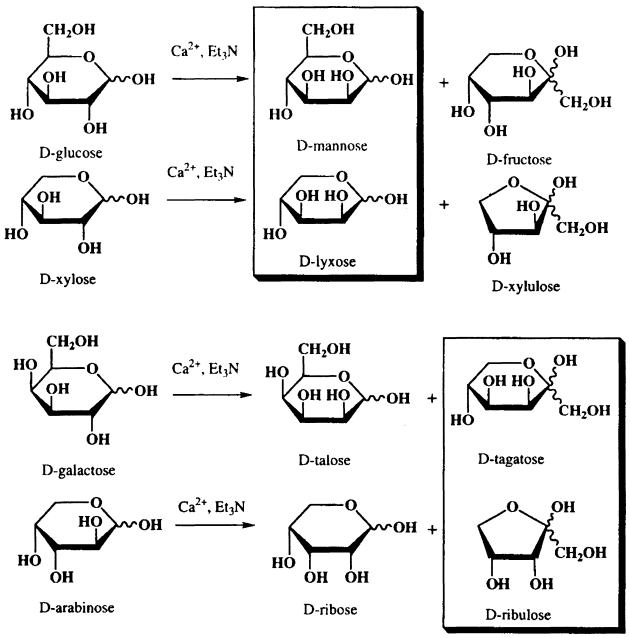

Scheme 3.

We have also examined C-2 epimerization of various disaccharides by using Ca^{2+}-monoamine systems. By employing this simple procedure, naturally rare (1→4)-linked heterodisaccharides having a D-mannose unit as the reducing terminal can be easily obtained from disaccharides with D-glucose unit as the reducing terminal, which are abundant in nature.

7. Antifungal Nickel(II) Complexes Derived from Amino Sugars against Pathogenic Yeast, *Candida albicans*[25]

There is increasing interest in the use of metal-containing compounds in medicine. Especially, the development of medically effective new compounds against the pathogenic yeast *Candida albicans* that causes serious disease in HIV-seropositive patients is highly desirable. It is well known that fungal cells including *C. albicans* need sugars as carbon sources for their growth. Sugar complexes are expected to be utilized by the fungal cells.

Figure 16 shows the growth inhibitory effect of Ni complexes ($[Ni(D\text{-}GlcN\text{-}en)_2]C1_2 \cdot H_2O$ (**9**·H_2O) and $[Ni(D\text{-}GlcN\text{-}tn)_2]C1_2 \cdot 4H_2O$ (**8**·$4H_2O$)) against a *C. albicans* strain, IFO1385, in the modified Sabouraud medium and in the standard Sabouraud medium. All compounds inhibited fungal growth in both media. The MIC (minimal concentration of inhibition) value of the inorganic compound $NiCl_2 \cdot 6H_2O$ was 0.2 mM. Compared to the inorganic compound, the sugar complexes and diamine complexes gave a higher MIC value (0.25 mM) in the modified medium as well as in the standard one. Thus the complexes showed effective antifungal activity, but the inhibitory effects on the fungal growth appeared to decrease slightly in comparison to the values for the inorganic compound. As far as the MIC values were concerned, no significant difference was detected between the two carbon sources. The complex gave one order higher MIC values than those of conventional antifungal agents, such as fluconazole.[73]

Cell morphology was examined by microscopy on the cultures containing each compound at concentrations around MIC. In the media containing the sugar complex at the concentrations of 0.2–0.8 mM, rounded yeast cells making clumps appeared in the standard Sabouraud media, or slightly bent cells making clumps appeared in the modified ones. These results indicated that these sugar complexes had the specific activity of inhibiting cell separation after bud growth rather than

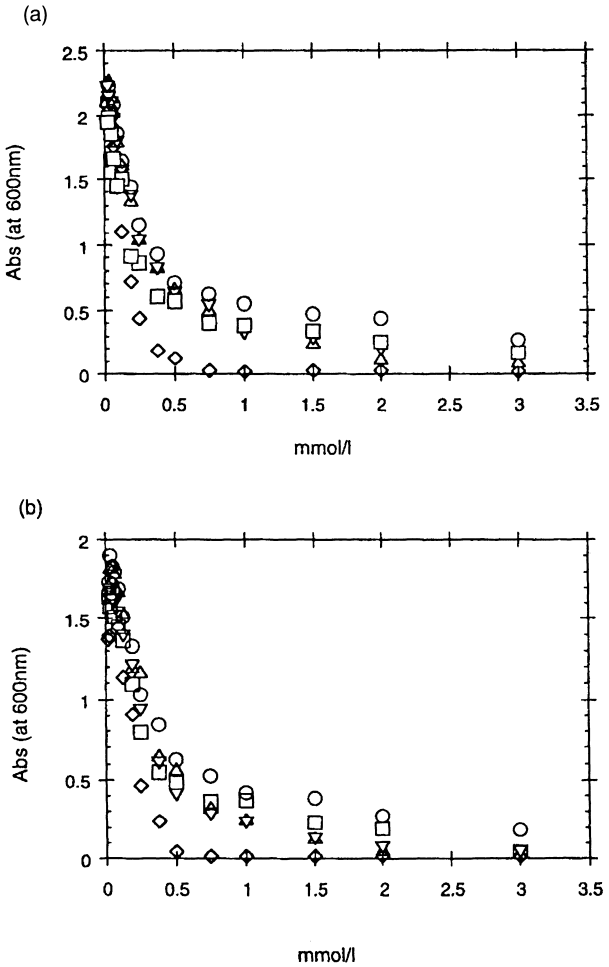

Fig. 16. Growth inhibitory effect of inhibitors against *C. albicans* at various concentration in the modified Sabouraud medium (a) and in the standard Sabouraud medium (b), (◇) $NiCl_2{\cdot}6H_2O$; (△) $[Ni(en)_3]Cl_2{\cdot}2H_2O$; (▽) $[Ni(tn)_3]$-$Cl_2{\cdot}2H_2O$; (○) $[Ni(\text{D-GlcN-en})_3]Cl_2{\cdot}2H_2O$; (□) $[Ni(\text{D-GlcN-tn})_3]Cl_2{\cdot}1.5H_2O$.

inhibiting cell proliferation at the concentrations around MIC. It is also of interest that morphological changes in individual cells driven by the complex depend on sugars which are used in each medium as the carbon source; however, the inhibitory effect on the process of cell separation by the sugar complex was apparently the same in both carbon sources.

The processes of forming budding septum and the following daughter cell-separation in yeast cells are under the control of both chitin synthesis and degradation.[74,75] The cell separation is facilitated by partial digestion of the chitin septum by a chitinase (chitin-degradation enzyme), and an inhibition of the chitinase activity results in non-separation of daughter cells and formation of cell clumps.[74,75]

Thus, we investigated chitinase inhibition by these sugar complexes. Initial velocities of chitinase-catalyzed hydrolysis of 4-methylumbelliferyl β-D-*N*,*N*′,*N*″-triacetylchitotrioside (4MUTAC) were determined by continuous monitoring of 4MU release, in samples containing various concentrations of the substrate (90–250 μM) and the inhibitor complexes **9** and **8** (0–1.0 mM). The Linewever–Burk plot analysis of these reactions suggested that the modes of inhibitions were competitive with inhibition constants (K_i = 1.3 mM for **9**, K_I = 1.8 mM for **8**). These K_i values were high, compared to the value of 0.23 μM that had been obtained for the allosamidine, a potent competitive inhibitor of *C. albicans* chitinase.[76] However, the sugar complexes were primarily intended to decrease the toxicity of the inorganic Ni, so the specificity of enzyme inhibition may be due to the structure of sugar moiety in the complexes. Although chitinase is widely distributed among plants, microorganisms, marine, invertebrates, ash, insects and marine bacteria, there are no known chitinase inhibitors except for allosamidin,[77] its derivatives,[78] and the styloguanidines.[79] Therefore, the present sugar complexes can be regarded as a candidate for developing a novel chitinase inhibitor.

8. Zinc(II) Complexes Containing *N*-Glycosides Derived from Ethylenediamine and D-Glucosamine[22]

Zinc is commonly found to bind to proteins in nature, either as a part of a catalytic site in enzymes[80] or as a structural component, as in DNA binding "zinc fingers".[81] Complexes of Zn(II) with monosaccharides Fru[82] (fructose) and GlupA (D-glucopyranosiduronic acid)[83] have been described, as has electrostatic binding to oligogalacturonates.[84] The binding of Zn(II) to heparin and glycosylaminoglycans was also reported.[85–88] Therefore, the ability to clarify the nature of the coordination behavior of sugars around the Zn(II) center is highly desirable. In this section, we describe the first successful isolation and X-ray crystal structure determination of zinc(II) complexes containing *N*-glycosides derived from D-glucosamine (D-GlcN) and ethylenediamine including their structure analysis in solution by means of ^1H and ^{13}C NMR measurements.

Zinc(II) complexes containing *N*-glycosides derived from D-glucosamine (D-GlcN) and ethylenediamine (en), $[Zn(\text{D-GlcN-en})_2]X_2$ (**30a** X = C1, **30b** $X_2 = SO_4^{2-}$), were prepared. A perspective drawing of the complex cation is given in Fig. 17. The complex cation of **30a** has nearly C_2 symmetry and the central zinc atom is octahedrally coordinated by two tridentate *N*-glycoside ligands from D-glucosamine and ethylenediamine. The *N*-glycoside ligand, D-GlcN-en, ligates to the zinc atom through the C2 amino nitrogen atom of D-glu-

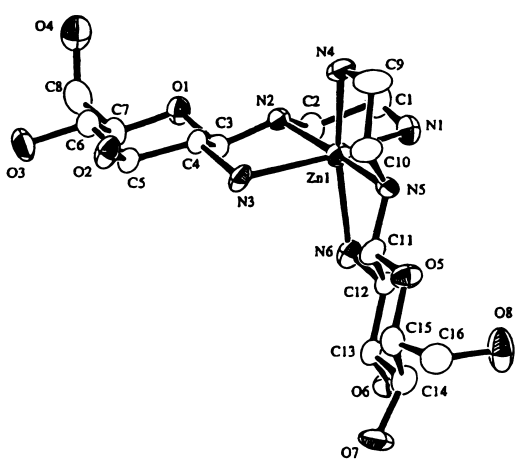

Fig. 17. Perspective drawing of $[Zn(\text{D-GlcN-en})_2]^{2+}$ with the atomic numbering scheme.

cosamine and the two nitrogen atoms of the diamine in a meridional mode with Δ configuration around the metal center defined by the two sugar chelate rings. The configuration around the metal center in **30a** is the same as that in [Ni(D-GlcN-en)$_2$]Cl$_2$ **9**.[31]

The analysis of the solution conformation of the sugar ring in **30a** based on vicinal coupling constants confirmed the similar structure revealed by X-ray crystallography as described below. The successful use of proton NMR spectroscopy for the elucidation of structural details in conformational analysis depends largely on the availability of a reliable functional relationship between vicinal proton-proton coupling constants and associated φ (H–C–C–H) torsional angles, usually refered to as a Karplus-type equation. In our previous paper,[49] we analyzed the structures of the sugar units of cobalt(Ⅲ) complexes containing an *N*-glycoside derived from ethylenediamine and an aldose by means of the semiempirical AMl calculations coupled with the conversion of the vicina1 ^{1}H–^{1}H spin–spin coupling constants in the ^{1}H NMR spectra into torsion angles of the corresponding H–C–C–H fragments, where we used the empirical Karplus-type equation proposed by Haasnoot et al.[89] Recently Altona et al. proposed an extended Karplus equation by considering empirical group electronegativities as described in Eq. 2,[90] where λ_i, are empirical group electronegativities (substituent parameters) and s_i stands for the 'sign factor' (formally denoted ξi) of the substituent attached to the H–C–C–H fragment in question, either +1 or −1.[89] The torsion angles were calculated for the H–C–C–H fragments on the sugar rings and diamine chelates from the atomic coordinates determined by the crystal structure of **30a**·2.75H$_2$O·0.5CH$_3$OH. The λ values defined in the literature[90] were used.

$$^3J(H_a,H_b) = 14.63\cos^2(\varphi) - 0.78\cos(\varphi) + 0.60 + \sum_i \lambda_i\{0.34 - 2.31[s_i(\varphi) + 18.4|\lambda_i|]\} \quad (2)$$

This generalized Karplus–Altona equation was effectively used in the recent reports on the anomeric effect in purine nucleotides[91] and vicinal coupling constants to H–C–C–F torsion angles.[92] The $^4C_1$ conformation of the pyranose rings in **30a** was confirmed by ^{1}H NMR spectroscopy and by using Eq. 2. The observed and calculated vicinal coupling constants in sugar ring of **30a** resemble each other corresponding to *trans* coupling. Therefore, it can be concluded that the hydrogens at C1, C2, C3, C4 and C5 are in the *trans* axial orientation corresponding to a β-$^4C_1$ conformation as revealed by X-ray crystallography.

9. (a) Convenient Synthesis of Sugar-Pendant Diamines[93–95]

The development of new sugar-pendant ligands with discrete metal binding sites is highly desirable. So far, we reported practical methods to synthesize sugar molecules derivatized with a polyamine in a one pot reaction in alcoholic solution via *N*-glycoside bond formation. Since these *N*-glycoside metal complexes are unstable in water, a new type of ligand is required for further investigation of a sugar-metal complex in aqueous solution.

Alkyl *O*-glycoside bonds are fairly stable under physiological conditions.[96,97] To develop a general methodology to prepare sugar based metal complexes, we describe the preparation of a novel set of chelating ligands possessing an *O*-glycoside bond that links the diamine moiety to a glycopyranose ring. The ligand library consists of 1,3-propanediamines, 1,2-ethylenediamines with a chiral center, and bisglucose-pendant 1,3-propanediamines (Fig. 18). The diamine moiety was connectd to the C1 carbon of the glycopyranose ring via an *O*-glycoside bond. The anomer configurations and sugar puckering conformations of many of these compounds were determined X-ray crystallographically from intermediate compounds such as the peracetylated diazide or dibromide.

1,3-Diamino-2-propyl D-glycopyranoside derivatives were synthesized from peracetylated sugar and 1,3-dibromo-2-propanol in four steps. D-Glucose, D-mannose, D-galactose, D-xylose, D-ribose, and maltose were employed as sugar molecules. In most cases, a single anomer, whose configuration depends on the configuration of the 2-acetoxy group (β-anomer for D-glucose, D-xylose, D-ribose, and maltose; α-anomer for D-mannose) was obtained by BF_3-catalyzed glycosidation of peracetylated glycopyranose with 1,3-dibromo-2-propanol; however, pentaacetyl-D-galactopyranose afforded mixures of the two anomers. The mixture was obtained owing to the participation of the 4-acetooxy group in addition to the normal 2-acetooxy neighboring group. This anomeric mixture was separated successfully by silica gel column chromatography after conversion to the diazido analogs with sodium azide.

Most of the diazides afford X-ray quality crystals after recrystallization. Structures of these precursors, as well as that of the dibromo precursor for D-ribose derivative were determined by X-ray crystallography. The NMR data of these compounds are in good agreement with these solid-state structures, indicating the similarity in sugar ring puckering in the solid and solution states. The crystal structure studies of the diazido or dibromo precursors provide useful information about the structure of the diamine derivatives because the procedures induce significant structural changes in neither the anomeric position nor the stereocenters, as determined by NMR investigations (vide supra).

In contrast to the 1,3-propanediamine compounds, use of an ethylenediamine moiety produces an asymmetric carbon at the point of attachment of the sugar (Fig. 18). Diastereomers of the diazido precurser were separated by recrystallization, in which the sugar molecules D-glucose and D-xylose which were

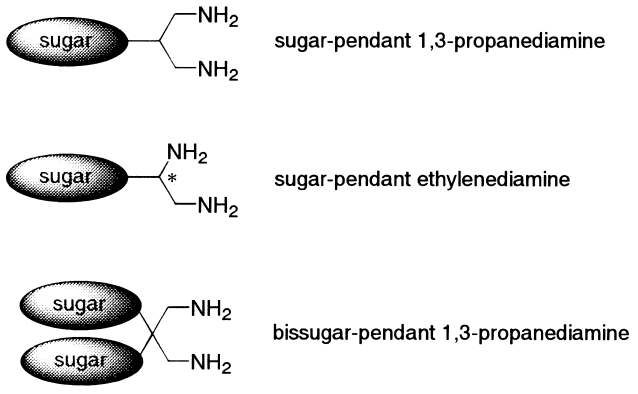

Fig. 18. Sugar-pendant diamines

utilized for this study act as a chiral auxiliary, giving rise to an optically pure sugar-pendant ethylenediamines. Bis(bromomethyl)bis(hydroxymethy1)methane gave bisglucose-pendant diamines.

Since the present method does not require chromatography, except for anomer separation in the case of D-galactose derivative, it is suitable for multigram syntheses of diamine-sugar ligands. Even though other routes are required in order to accomplish the preparation of a complete set of anomers and chiral diastereomers with the ethylenediamine derivatives, this method is useful for preparation of diamine-sugar hybrid molecules. The metal binding properties of these compounds were investigated.[98]

9. (b) Unprecedented Sugar-Dependent In Vivo Antitumor Activity of Carbohydrate-Pendant *cis*-Diamminedichloroplatinum(II) Complexes[23]

Cisplatin (*cis*-diamminedichloroplatinum(II), *cis*-DDP) is an effective anticancer drug. It binds to DNA after loss of its chloride leaving groups by aquation and/or hydrolysis. Cisplatin induces significant bends into the DNA structure upon binding to the N7 atoms of guanine bases of the d(GpG) sequence. The recognition of these bent structures by high-mobility group (HMG) proteins is believed to play an important role in the anticancer activity of cisplatin.[99–101] Because the importance of the interactions between carbohydrates and proteins is well known, the construction of carbohydrate-cisplatin conjugates[36,51,102,103] is of significant interest. Thus we reported a systematic synthesis of carbohydrate-pendant cisplatin derivatives and their in vivo antitumor activity.

Eight carbohydrate-pendant platinum(II) complexes (Fig. 19) have been synthesized from K_2PtCl_4 and the corresponding carbohydrate–diamine conjugate in aqueous solution. D-Glucose, D-mannose, D-galactose, D-xylose, and L-glucose are attached to the dichloroplatinum(II) moiety by 1,3- or 1,2-diaminopropane chelates through with an *O*-glycoside bond. This series of compounds includes the α and β anomers for the D-galactose derivative (**33** and **34**), the D and L isomers for the glucose derivative with a chiral 1,2-diaminopropane linker (**36** and **37**), and both six and five membered chelate ring size isomers with D-glucose (**31** and **36**) and D-xylose (**35** and **38**). All of the compounds had NMR, CD, MS, and elemental analyses consistent with their proposed structures.

The anticancer activity of these platinum(II) complexes was investigated against P388 cells implanted in mice. Cancer cells (10^6 of P388 cell) were transplanted intraperitoneally (ip) into CDF1 mice (6 mice/group), followed by ip administration of the drugs to the mice on days 1 and 5. The mean survival time of the treated group (*T*) was compared with that of the untreated control group (*C*) (Fig. 20). A *T*/*C* value of 194% was obtained for the α-D-galactose derivative **33** at 400-mg/kg dose, whereas the β-D-galactose derivative **34** showed low toxicity at the same dose. Significant toxicity was observed for the mannose derivative **32**, even at a dose of 100 mg/kg. Because the LD_{50} of cisplatin is approximately 10 mg/kg,[36,51] all the carbohydrate moieties reduced the toxicity inherent with platinum(II) complexes significantly. The linker structure also affects the antitumor activity of **31** versus **36**, or **35** versus **38**; however, D- and L-glucose derivatives (**36**,**37**) showed similar

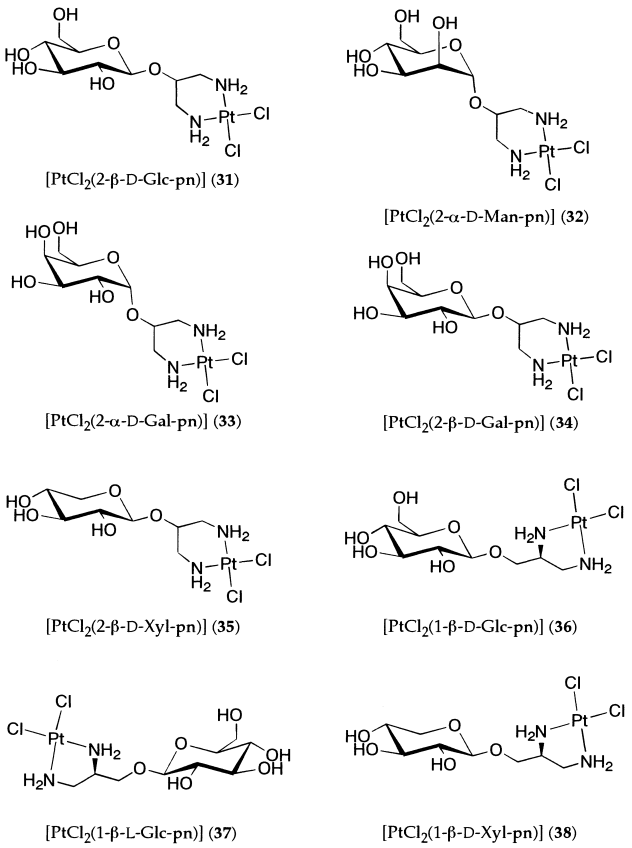

Fig. 19. Structures of platinum(II) complexes **31**–**38**.

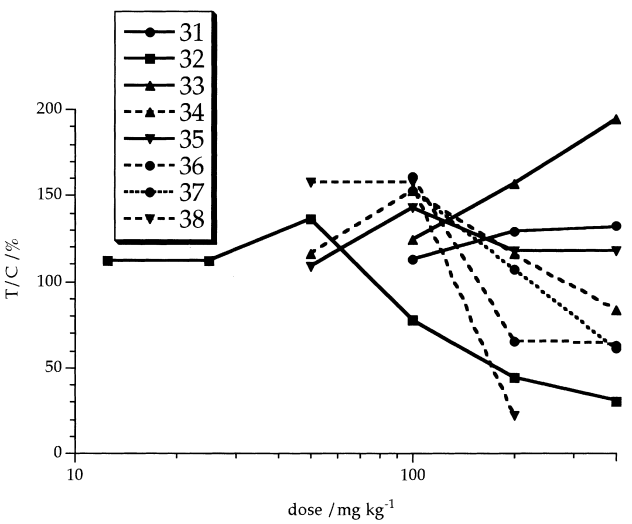

Fig. 20. Antitumor activity of carbohydrate-pendant platinum(II) complexes **31**–**38**.

dose/activity profiles.

Selective uptake in cancer cells or specific interaction between drug-damaged DNA and recognition protein may cause the difference in antitumor activity of these complexes. Another possible explanation is the pro-drug hypothesis, according to which all carbohydrate-pendant platinum(II) complexes have poor cell-membrane permeation properties. Selective hy-

drolysis of the carbohydrate moiety in the blood stream to generate the active drug may explain the sugar-dependent antitumor activity. This hypothesis may correspond to the reducing effect of cytotoxicity of the platinum complexes by sugar moiety. These data suggest that the appropriate carbohydrate and/or linker increases the clinical activity of carbohydrate-pendant platinum(II) complexes.

10. Concluding Remarks

In this account, we have introduced our recent studies of the synthesis, characterizations and stereochemistry of the transition metal complexes containing glycosylamines derived from sugar molecules and polyamines, the results of which suggested that the stereostructure of the sugar complexes can be modified by varying amines and metal ions used. Some practical applications of sugar–metal complexes are also described. Included are some intelligent sugar complexes having ion recognition ability that could be regarded as a new induced fit model in the enzymatic reaction, novel sugar transformation reactions promoted by a cooperative effects of calcium ion and monoamines, antifungal nickel(II) complexes derived from amino sugars, and unprecedented sugar-dependent in vivo antitumor activity of carbohydrate-pendant *cis*-platinum(II) complexes. However, we have made only slight progress to understanding the complicated interactions between biologically important carbohydrates and metal ions and their bioactivity. From these results, we would like to continue our study, hoping to design the highly functional glycoconjugated hybrid compounds.

The authors express our hearty appreciation to Professor Tomoaki Tanase, Professor Takahito Suzuki, Professor Masahiro Mikuriya, Professor Isamu Kinoshita, Professor Chris Orvig, and Dr. Makoto Obata for their great supports to this work and their helpful discussions. S. Y. also would like to thank students of our laboratories for their help for this work. This work was supported by a Grant-in-Aid for Scientific research from the Ministry of Education, Science, Sports and Culture and Japan Society for the Promotion of Science and by the Grant from the San-Ei Gen Foundation for Food Chemical Research. The authors thank the Cancer Chemotherapy Center (Japanese Foundation for Cancer Research) for the antitumor activity test.

References

1 J. A. Rendleman Jr., *Adv. Carbohydr. Chem.*, **21**, 209 (1966).

2 S. J. Angyal, *Pure Appl. Chem.*, **35**, 131 (1973).

3 S. J. Angyal, *Adv. Carbohydr. Chem. Biochem.*, **47**, 1 (1989).

4 J. F. Verchere, S. Capelle, F. Xin, and D. C. Crans, *Prog. Inorg. Chem. Biochem.*, **47**, 837 (1998).

5 Y. E. Alekseev, A. D. Garnovskii, and Y. A. Zhdanov, *Usp. Khim.*, **67**, 723 (1998).

6 D. M. Whitfield, S. Stojkovski, and B. Sarker, *Coord. Chem. Rev.*, **122**, 171 (1993).

7 U. Piarulli and C. Floriani, *Prog. Inorg. Chem.*, **45**, 393 (1997).

8 B. Gyurcsik and L. Nagy, *Coord. Chem. Rev.*, **203**, 81 (2000).

9 D. Steinborn, and H. Junicke, *Chem. Rev.*, **100**, 4283 (2000).

10 S. Yano, *Coord. Chem. Rev.*, **92**, 113 (1988).

11 S. Yano, and K. Ohtsuka, "Metal Ions in Biological Systems," Marcel dekker, Inc. (1996) p.27.

12 T. Tanase, M. Doi, R. Nouchi, M. Kato, Y. Sato, K. Ishida, K. Kobayashi, T. Sakurai, Y. Yamamoto, and S. Yano, *Inorg. Chem.*, **35**, 4848 (1996).

13 T. Tanase, Y. Yasuda, T. Onaka, and S. Yano, *J. Chem. Soc., Dalton Trans.*, **1998**, 345.

14 S. Yano, M. Doi, M. Kato, I. Okura, T. Nagano, Y. Yamamoto, and T. Tanase, *Inorg. Chim. Acta*, **249**, 1 (1996).

15 T. Tanase, M. Nakagoshi, A. Teratani, M. Kato, I. Yamamoto, and S. Yano, *Inorg. Chem.*, **33**, 5 (1994).

16 S. Yano, M. Nakagoshi, A. Teratani, M. Kato, T. Onaka, M. Iida, T. Tanase, Y. Yamamoto, H. Uekusa, and Y. Ohashi, *Inorg. Chem.*, **36**, 4187 (1997).

17 T. Tanase, T. Onaka, M. Nakagoshi, I. Kinoshita, K. Shibata, M. Doe, J. Fujii, and S. Yano, *Chem. Commun.*, **1997**, 2115.

18 T. Tanase, T. Onaka, M. Nakagoshi, I. Kinoshita, K. Shibata, M. Doe, J. Fujii, and S. Yano, *Inorg. Chem.*, **38**, 3150 (1999).

19 S. Yano, M. Doi, S. Tamakoshi, W. Mori, M. Mikuriya, A. Ichimura, I. Kinoshita, Y. Yamamoto, and T. Tanase, *Chem. Commun.*, **1997**, 997.

20 T. Tanase, S. Tamakoshi, M. Doi, W. Mori, and S. Yano, *Inorg. Chim. Acta*, **266**, 5 (1997).

21 T. Tanase, S. Tamakoshi, M. Doi, M. Mikuriya, H. Sakurai, and S. Yano, *Inorg. Chem.*, **39**, 692 (2000).

22 S. Yano, S. Inoue, Y. Yasuda, T. Tanase, Y. Mikata, T. Kakuchi, T. Tsubomura, M. Yamasaki, I. Kinoshita, and M. Doe, *J. Chem. Soc., Dalton Trans.*, **1999**, 1851.

23 T. Tanase, T. Takei, M. Hidai, and S. Yano, *Carbohydr. Res.*, **333**, 303 (2001).

24 S. Yano, S. Inoue, R. Nouchi, M. Kato, and T. Suzuki, *Biol. Pharm. Bull.*, **18**, 923 (1995).

25 S. Yano, S. Inoue, R. Nouchi, K. Mogami, Y. Shinohara, Y. Yasuda, M. Kato, T. Tanase, T. Kakuchi, Y. Mikata, T. Suzuki, and Y. Yamamoto, *J. Inorg. Biochem.*, **69**, 15 (1998).

26 Y. Mikata, Y. Shinohara, K. Yoneda, Y. Nakamura, I. Brudziñska, T. Tanase, T. Kitayama, R. Takagi, T. Okamoto, I. Kinoshita, M. Doe, C. Orvig, and S. Yano, *Bioorg. Med. Chem. Lett.*, **11**, 3045 (2001).

27 S. Takizawa, H. Sugita, S. Yano, and S. Yoshikawa, *J. Am. Chem. Soc.*, **102**, 7969 (1980).

28 T. Tsubomura, S. Yano, S. Yoshikawa, K. Toriumi, and T. Ito, *Polyhedron*, **2**, 123 (1983).

29 H. Shioi, S. Yano, K. Toriumi, T. Ito, and S. Yoshikawa, *Chem. Commun.*, **1983**, 201.

30 T. Tsubomura, S. Yano, K. Toriumi, T. Ito, and S. Yoshikawa, *Bull. Chem. Soc. Jpn.*, **57**, 1833 (1984).

31 S. Yano, Y. Sakai, K. Toriumi, T. Ito, H. Ito, and S. Yoshikawa, *Inorg. Chem.*, **24**, 498 (1985).

32 S. Yano, S. Takizawa, H. Sugita, T. Takahashi, H. Shioi, T. Tsubomura, and S. Yoshikawa, *Carbohydr. Res.*, **142**, 179 (1985).

33 T. Tsubomura, S. Yano, K. Toriumi, T. Ito, and S. Yoshikawa, *Inorg. Chem.*, **24**, 3218 (1985).

34 T. Tanase, K. Kurihara, S. Yano, K. Kobayashi, T. Sakurai,

and S. Yoshikawa, *Chem. Commun.*, **1985**, 1562.
35 T. Tsubomura, S. Yano, and S. Yoshikawa, *Inorg. Chem.*, **25**, 392 (1986).
36 T. Tsubomura, S. Yano, K. Kobayashi, T. Sakurai, and S. Yoshikawa, *Chem. Commun.*, **1986**, 459.
37 T. Tanase, F. Shimizu, S. Yano, and S. Yoshikawa, *Chem. Commun.*, **1986**, 1001.
38 K. Ishida, S. Yano, and S. Yoshikawa, *Inorg. Chem.*, **25**, 3552 (1986).
39 T. Tanase, F. Shimizu, M. Kuse, S. Yano, S. Yoshikawa, and M. Hidai, *Chem. Commun.*, **1987**, 659.
40 T. Tanase, F. Shimizu, S. Yano, M. Hidai, S. Yoshikawa, and K. Asakura, *Nippon Kagaku Kaishi*, **1987**, 322.
41 T. Takahashi, S. Yano, S. Yoshikawa, and M. Hidai, *Nippon Kagaku Kaishi*, **1987**, 328.
42 T. Tanase, T. Murata, S. Yano, M. Hidai, and S. Yoshikawa, *Chem. Lett.*, **1987**, 1409.
43 T. Tanase, K. Kurihara, S. Yano, K. Kobayashi, T. Sakurai, S. Yoshikawa, and M. Hidai, *Inorg. Chem.*, **26**, 3134 (1987).
44 S. Yano, T. Takahashi, Y. Sato, K. Ishida, T. Tanase, M. Hidai, K. Kobayashi, and T. Sakurai, *Chem. Lett.*, **1987**, 2153.
45 T. Tanase, K. Ishida, T. Watanabe, M. Komiyama, K. Koumoto, S. Yano, M. Hidai, and S. Yoshikawa, *Chem. Lett.*, **1988**, 327.
46 K. Ishida, M. Yashiro, S. Yano, M. Hidai, and S. Yoshikawa, *J. Am. Chem. Soc.*, **110**, 2015 (1988).
47 T. Tsubomura, S. Yano, and S. Yoshikawa, *Bull. Chem. Soc. Jpn.*, **61**, 3497 (1988).
48 T. Tanase, F. Shimizu, M. Kuse, S. Yano, M. Hidai, and S. Yoshikawa, *Inorg. Chem.*, **27**, 4085 (1988).
49 K. Ishida, S. Nonoyama, T. Hirano, S. Yano, M. Hidai, and S. Yoshikawa, *J. Am. Chem. Soc.*, **111**, 1599 (1989).
50 K. Ishida, M. Yashiro, S. Yano, M. Hidai, and S. Yoshikawa, *J. Chem. Soc., Dalton Trans.*, **1989**, 1241.
51 T. Tsubomura, M. Ogawa, S. Yano, K. Kobayashi, T. Sakurai, and S. Yoshikawa, *Inorg. Chem.*, **29**, 2622 (1990).
52 T. Takei, T. Tanase, S. Yano, and M. Hidai, *Chem. Lett.*, **1991**, 1629.
53 T. Tanase, T. Takei, M. Hidai, and S. Yano, *J. Chem. Res.*, **1992**, 252.
54 S. Yano, M. Kato, H. Shioi, T. Takahashi, T. Tsubomura, K. Toriumi, T. Ito, M. Hidai, and S. Yoshikawa, *J. Chem. Soc., Dalton Trans.*, **1993**, 1699.
55 T. Tanase, R. Nouchi, M. Kato, N. Nakamura, T. Yamamura, Y. Yamamoto, and S. Yano, *J. Chem. Soc., Dalton Trans.*, **1993**, 2645.
56 L. Sacconi, *Transition Met. Chem.*, **4**, 199 (1968).
57 W. Z. Ebeling, *Phys. Chem. (Leipzig)*, **238**, 400 (1968).
58 H. Yokoyama and H. Yamatera, *Bull. Chem. Soc. Jpn.*, **48**, 1770, 3002 (1975).
59 E. I. Solomon, F. Tuczek, D. E. Root, and C. A. Brown, *Chem. Rev.*, **94**, 827 (1994).
60 J. Jenkins, J. Janin, F. Rey, M. Chiadmi, H. Tilbeurgh, I. Lasters, M. D. Maeyer, D. V. Belle, S. J. Wodak, M. Lauwereys, P. Stannsenns, N. T. Mrabet, J. Snauwaert, G. Matthyssens, and A.-M. Lambeir, *Biochemistry*, **31**, 5449 (1992).
61 M. Whitlow, A. J. Howard, B. C. Finzel, T. L. Poulos, E. Winborne, and G. L. Gilliland, *Proteins*, **9**, 153 (1991).
62 Y. Zhang, J.-Y. Liang, S. Huang, H. Ke, and W. N. Lipscomb, *Biochemistry*, **32**, 17 (1993).
63 Y. Xue, S. Huang, J.-Y. Liang, Y. Zhang, and W. N. Lipscomb, *Proc. Natl. Acad. Sci., U.S.A.*, **91**, 12482 (1994).
64 K. D. Hardman, R. C. Agarwal, and M. Freister, *J. Mol. Biol.*, **157**, 69 (1982).
65 K. Kambe, *J. Phys. Soc. Jpn.*, **5**, 48 (1950).
66 D. W. Allen, I. W. Nowell, and B. F. Taylor, *J. Chem. Soc., Dalton Trans.*, **1985**, 2505.
67 M. J. Baldwin, J. W. Kampf, M. L. Kirk, and V. L. Pecoraro, *Inorg. Chem.*, **34**, 5252 (1995).
68 W. I. Weis, K. Drickamer, and W. A. Hendrickson, *Nature*, **360**, 127 (1992).
69 K. K.-S. Ng and W. I. Weis, *Biochemistry*, **36**, 979 (1997).
70 L. Poppe, G. S. Brown, J. S. Philo, P. V. Nikrad, and B. H. Shah, *J. Am. Chem. Soc.*, **119**, 1727 (1997).
71 J. W. Becker, J. G. N. Reeke, J. L. Wang, B. A. Cunningham, and G. M. Edelman, *J. Biol. Chem.*, **260**, 1513 (1975).
72 M. L. Hays, N. J. Pennings, A. S. Serianni, and A. S. Barker, *J. Am. Chem. Soc.*, **104**, 6764 (1982).
73 T. E. Rogers and J. N. Galgiani, *Antimicrob. Ag. Chemother.*, **30**, 418 (1986).
74 M. I. Kuranda, and P. W. Robbins, *J. Biol. Chem.*, **266**, 19758 (1991).
75 E. Cabib, S. J. Silverman, and J. A. Shaw, *Gen. Microbiol.*, **138**, 97 (1992).
76 K. Dickinson, V. Keer, C. A. Filitchcock, and D. J. Adams, *J. Gen. Microbiol.*, **135**, 1417 (1989).
77 S. Sakuda, A. Isogai, S. Miyamoto, and A. Suzuki, *Tetrahedron Lett.*, **27**, 2475 (1986).
78 M. Kinoshita, S. Sakuda, and Y. Yamada, *Biosci, Biotech. Biochem.*, **57**, 1699 (1993).
79 T. Kato, S. Shizuri, H. Izumida, A. Yokoyama, and M. Endo, *Tetrahedron Lett.*, **36**, 2133 (1995).
80 B. Sarker, "Metal Protein Interactions: Progress in Food and Nutritional Sciences," Pergamon, Oxford (1987) p.363.
81 J. M. Berg, *J. Biol. Chem.*, **265**, 6513 (1990).
82 H. A. T. Riahi, *Carbohydr. Res.*, **172**, 1 (1988).
83 H. A. T. Riahi, *J. Inorg. Biochem.*, **265**, 23 (1986).
84 J. Ollis, V. J. James, S. J. Angyal, and P. M. Pojer, *Carbohydr. Res.*, **60**, 219 (1978).
85 E. Grushka and A. S. Cohen, *Anal. Lett.*, **15**, 1277 (1982).
86 R. F. Parrish and W. R. Fair, *Biochem. J.*, **193**, 407 (1981).
87 N. A. Woodhead, W. F. Long, and F. B. Williamson, *Biochem. J.*, **237**, 281 (1986).
88 C. S. Sato, and F. Gyorkey, *J. Biochem.*, **80**, 883 (1976).
89 C. A. G. Haasnoot, F. A. A. M. De Leeuw, and C. Altona, *Tetrahedron*, **36**, 2783 (1980).
90 C. Altona, R. Francke, R. D. Haan, J. H. Ippel, G. J. Daalmans, A. J. A. W. Hoekzema, and J. V. Wijk, *J. Magn. Reson.*, **32**, 670 (1994).
91 M. Polak, B. Mohar, J. Kobe, and J. Plavec, *J. Am. Chem. Soc.*, **120**, 2508 (1998).
92 C. Thibaudeau, J. Plavec, and J. Chattopadhyaya, *J. Org. Chem.*, **63**, 4967 (1998).
93 Y. Mikata, K. Yoneda, T. Tanase, I. Kinoshita, M. Doe, F. Nishida, K. Mochida, and S. Yano, *Carbohydr. Res.*, **313**, 175 (1998).
94 Y. Mikata, Y. Shinohara, K. Yoneda, Y. Nakamura, K. Esaki, M. Tanahashi, I. Brudzinska, S. Hirohara, M. Yokoyama, K. Mogami, T. Tanase, T. Kitayama, K. Takashiba, K. Nabeshima, R. Takagi, M. Takatani, T. Okamoto, I. Kinoshita, M. Doe, A. Hamazawa, M. Morita, F. Nishida, T. Sakakibara, C. Orvig, and S.

Yano, *J. Org. Chem.*, **66**, 3783 (2001).
95 S. Yano, Y. Shinohara, K. Mogami, M. Yokoyama, T. Tanase, T. Sakakibara, F. Nishida, K. Mochida, I. Kinoshita, M. Doe, K. Ichihara, Y. Naruta, P. Mehrkhodavandi, P. Buglyó, B. Song, C. Orvig, and Y. Mikata, *Chem. Lett.*, **1999**, 255.
96 "Chemistry of *O*-Glycosideic Bond: Formation & Cleavage," ed by A. F. Bochkov and G. E. Zaikov, Pergamon Press, Oxford (1979).
97 B. Capon, *Chem. Rev.*, **69**, 407 (1969).
98 B. Song, P. Mehrkhodavandi, P. Buglyó, Y. Mikata, Y. Shinohara, K. Yoneda, S. Yano, and C. Orvig, *J. Chem. Soc., Dalton Trans.*, **2000**, 1325.
99 E. R. Jamieson and S. J. Lippard, *Chem. Rev.*, **99**, 2467 (1999).
100 Q. He, U.-M. Ohndorf, and S. J. Lippard, *Biochemistry*, **39**, 14426 (2000).
101 Q. He, C. H. Liang, and S. J. Lippard, *Proc Natl. Acad. Sci., U.S.A*, **97**, 5768 (2000).
102 S. Hanessian and J. Wang, *Can. J. Chem.*, **71**, 886 (1993).
103 Y. Chen, M. J. Heeg, P. G. Braunschweiger, W. Xie, and P. G. Wang, *Angew. Chem., Int. Ed.*, **38**, 1768 (1999).

Shigenobu Yano was born in 1945 in Nagano Prefecture, Japan. He received his B. of Science degree in 1967, his M. of Science degree in 1969, and his Ph.D. in 1972 from Tohoku University. He was a research associate, a lecturer, an assistant Professor of the Department of Synthetic Chemistry, Faculty of Engineering, the University of Tokyo from 1972 to 1988. He became a Professor of the Department of Chemistry, Faculty of Science, Nara Women's University in 1988. He is now Professor of Division of Material Science, Graduate School of Human Culture, Nara Women's University. Dr. Yano's research interests include synthetic chemistry, coordination chemistry, bioinorganic chemistry. Recently, he feels particular interest in functional hybrid metal complexes. He received the Divisional Award (Inorganic Chemistry) of the Chemical Society of Japan in 1989.

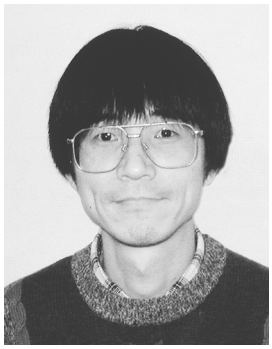

Yuji Mikata was born in 1965 in Osaka Prefecture, Japan. He received his B. of Science degree from Kobe University in 1988. He received his M. of Science degree and Ph.D. from Kyoto University in 1990 and 1993, respectively. He was a JSPS pre- and postdoctoral Fellow during 1992–1993 at Kyoto University, then he was appointed to be a Research Associate of the Department of Chemistry, Nara Women's University. He experienced a research Fellowship at MIT (Professor S. J. Lippard) in the period of 1999–2001 as a JSPS postdoctral Fellow for research abroad. He is an Associate Professor of KYOUSEI Science Center, Nara Women's University from 2001. His research interests are bioorganic and bioinorganic chemistry, especially development of bioactive small molecules.